(19) Europäisches Patentamt
European Patent Office
Office européen des brevets

(11) **EP 4 172 784 B1**

(12) **EUROPEAN PATENT SPECIFICATION**

(45) Date of publication and mention of the grant of the patent:
02.04.2025 Bulletin 2025/14

(21) Application number: **20942544.6**

(22) Date of filing: **23.12.2020**

(51) International Patent Classification (IPC):
H10N 50/10 *(2023.01)* ***H10N 50/80*** *(2023.01)*
H10N 50/85 *(2023.01)* ***G11C 11/18*** *(2006.01)*
G11C 11/16 *(2006.01)* ***H03B 15/00*** *(2006.01)*
G11B 5/00 *(2006.01)*

(52) Cooperative Patent Classification (CPC):
H10N 50/85; G11C 11/161; G11C 11/18; H03B 15/006; H10N 50/10; H10N 50/80;
G11B 2005/0024

(86) International application number:
PCT/US2020/066902

(87) International publication number:
WO 2022/005518 (06.01.2022 Gazette 2022/01)

(54) BISMUTH ANTIMONY ALLOYS FOR USE AS TOPOLOGICAL INSULATORS

WISMUT-ANTIMON-LEGIERUNGEN ZUR VERWENDUNG ALS TOPOLOGISCHE ISOLATOREN

ALLIAGES DE BISMUTH ET D'ANTIMOINE DESTINÉS À ÊTRE UTILISÉS COMME ISOLANTS TOPOLOGIQUES

(84) Designated Contracting States:
AL AT BE BG CH CY CZ DE DK EE ES FI FR GB GR HR HU IE IS IT LI LT LU LV MC MK MT NL NO PL PT RO RS SE SI SK SM TR

(30) Priority: **30.06.2020 US 202016917334**

(43) Date of publication of application:
03.05.2023 Bulletin 2023/18

(73) Proprietor: **Western Digital Technologies, Inc.**
San Jose, CA 95119 (US)

(72) Inventors:
- **YORK, Brian, R.**
  San Jose, California 95119 (US)
- **HWANG, Cherngye**
  San Jose, California 95119 (US)
- **SPOOL, Alan**
  San Jose, California 95119 (US)
- **GRIBELYUK, Michael**
  San Jose, California 95119 (US)
- **LE, Quang**
  San Jose, California 95119 (US)

(74) Representative: **Murgitroyd & Company**
165-169 Scotland Street
Glasgow G5 8PL (GB)

(56) References cited:
US-A1- 2014 254 252 **US-A1- 2017 288 666**
US-B2- 9 929 210

- **KHANG NGUYEN HUYNH ET AL: "A conductive topological insulator with large spin Hall effect for ultralow power spin-orbit torque switching", NATURE MATERIALS, vol. 17, no. 9, 30 July 2018 (2018-07-30), pages 808 - 813, XP036572906, ISSN: 1476-1122, [retrieved on 20180730], DOI: 10.1038/S41563-018-0137-Y**
- **KHANG NGUYEN HUYNH DUY ET AL: "A conductive topological insulator with large spin Hall effect for ultralow power spin-orbit torque switching - Supplementary Information", NATURE MATERIALS, 30 July 2018 (2018-07-30), XP093095034, Retrieved from the Internet <URL:https://static-content.springer.com/esm/art%3A10.1038%2Fs41563-018-0137-y/MediaObjects/41563_2018_137_MOESM1_ESM.pdf> [retrieved on 20231025], DOI: 10.1038/s41563-018-0137-y**

Processed by Luminess, 75001 PARIS (FR)

(Cont. next page)

- TOKURA YOSHINORI ET AL: "Magnetic topological insulators", NATURE REVIEWS PHYSICS, vol. 1, no. 2, 1 February 2019 (2019-02-01), pages 126 - 143, XP093094925, DOI: 10.1038/s42254-018-0011-5
- NGUYEN HUYNH DUY KHANG; YUGO UEDA; PHAM NAM HAI: "A conductive topological insulator with colossal spin Hall effect for ultra-low power spin-orbit-torque switching", ARXIV.ORG, CORNELL UNIVERSITY LIBRARY, 201 OLIN LIBRARY CORNELL UNIVERSITY ITHACA, NY 14853, 22 September 2017 (2017-09-22), 201 Olin Library Cornell University Ithaca, NY 14853 , XP081401042, DOI: 10.1038/s41563-018-0137-y
- YABIN FAN, PRAMEY UPADHYAYA, XUFENG KOU, MURONG LANG, SO TAKEI, ZHENXING WANG, JIANSHI TANG, LIANG HE, LI-TE CHANG, MOHAMMAD MONTA: "Magnetization switching through giant spin–orbit torque in a magnetically doped topological insulator heterostructure", NATURE MATERIALS, NATURE PUBLISHING GROUP UK, LONDON, vol. 13, no. 7, 1 July 2014 (2014-07-01), London, pages 699 - 704, XP055593241, ISSN: 1476-1122, DOI: 10.1038/nmat3973

Description

CROSS-REFERENCE TO RELATED APPLICATIONS

[0001] This application claims priority to U.S. Application No. 16/917,334, filed June 30, 2020.

BACKGROUND OF THE DISCLOSURE

Field of the Disclosure

[0002] Embodiments of the present disclosure generally relate to bismuth antimony (BiSb) alloys with (012) orientation for use as topological insulators.

Description of the Related Art

[0003] BiSb with (012) orientation is a narrow gap topological insulator with both giant spin Hall effect and high electrical conductivity. BiSb is a material that has been proposed in various spin-orbit torque (SOT) applications, such as for a spin Hall layer for magnetoresistive random access memory (MRAM) devices and energy-assisted magnetic recording (EAMR) write heads.

[0004] However, BiSb materials have yet to be adopted in commercial SOT applications due to several obstacles. For example, BiSb materials have low melting points, large grain sizes, significant Sb migration issues upon thermal annealing due to its film roughness, difficulty maintaining a (012) orientation for maximum spin Hall effect and are generally soft and easily damaged by ion milling.

[0005] Therefore, there is a need for an improved SOT device and process of forming a BiSb layer with (012) orientation.

SUMMARY OF THE DISCLOSURE

[0006] The invention is a device as defined in the appended independent claim 1. Embodiments of the present invention generally relate to bismuth antimony (BiSb) alloys with (012) orientation for use as topological insulators in spin-orbit torque (SOT) devices as defined by the subject matter of the claims.

[0007] US2017/0288666 A1 describes voltage-controlled magnetic based devices that include a magnetic insulator; a topological insulator adjacent the magnetic insulator; and magnetic dopants within the topological insulator. The magnetic dopants are located within an edge region of the topological insulator to inhibit charge current flow in the topological insulator during a switching operation using an applied electric field generating by applying a switching voltage across two electrodes at opposite sides of the topological insulator. Power dissipation due to carrier-based currents can be avoided or at least minimized by the magnetic dopants at the edges of the topological insulator.

[0008] KHANG et al. describe in the article entitled "Conductive Topological Insulator With Large Spin Hall Effect For Ultralow Power Spin-Orbit Torque Switching", Nature Materials 17, 808-813 (2018), spin-orbit torque switching using the spin Hall effect in heavy metals and topological insulators.

[0009] In an article entitled "Magnetic Topological Insulators", Nature Reviews Physics 1, 126-143 (2019), TOKURA *et al.* review the basic concepts of magnetic topological insulators and their experimental realization, together with the discovery and verification of their emergent properties. In particular, they discuss how the development of tailored materials through heterostructure engineering has made it possible to access the quantum anomalous Hall effect, the topological magnetoelectric effect, the physics related to the chiral edge states that appear in these materials and various spintronic phenomena.

BRIEF DESCRIPTION OF THE DRAWINGS

[0010] So that the manner in which the above-recited features of the present disclosure can be understood in detail, a more particular description of the disclosure, briefly summarized above, may be had by reference to examples, some of which are illustrated in the appended drawings. It is to be noted, however, that the appended drawings illustrate only typical embodiments of this invention and examples and are therefore not to be considered limiting of its scope, for the invention may admit to other equally effective embodiments.

FIGS. 1A-1C are schematic illustration of a BiSb alloy layer comprising dopant element(s).

FIGS. 2A-2B are schematic illustrations of a BiSbE alloy layer comprising multiple BiSb lamellae layers and comprising dopant element lamellae layers between each of the BiSb lamellae layers. FIGS. 2C-2D are schematic illustrations of a BiSbE alloy layer comprising multiple BiSb lamellae layers and comprising dopant element lamellae

layers at the bottom edge and the top edge of the BiSbE alloy layer. FIGS. 2E-2F are schematic illustrations of a BiSbE alloy layer comprising multiple BiSb lamellae layers and comprising dopant element lamellae layers at the bottom edge, the center, and the top edge of the BiSbE alloy layer. FIGS. 2G-2H are schematic illustrations of a BiSbE alloy layer comprising multiple BiSb lamellae layers and comprising dopant element lamellae layers at the bottom edge of the BiSbE alloy layer.

FIG. 3 shows 2-theta XRD scans vs. logarithm of the intensity of the BiSb orientation of various stacks of BiSbE alloy layers comprising a non-metallic dopant element of Si.

FIG. 4 shows 2-theta XRD scans vs. logarithm of the intensity of the BiSb orientation of various stacks of BiSbE alloy layers comprising a metallic dopant element of CuAgNi.

FIG. 5 shows TOF-SIMS net intensity for dopant E-Cs+ clusters across the BiSbE alloy layer for dopant elements of NiFe, Si, and CuAgNi.

FIG. 6 shows TEM Cu EELS scans across a BiSbE stack comprising a silicide cap layer, a BiSbE alloy layer comprising a metallic dopant of CuAgNi, and a silicide seed layer.

FIG. 7 shows the conductivity versus thickness of various BiSbE alloy layers comprising a metallic dopant.

FIG. 8 shows the conductivity versus thickness of various BiSbE alloy layers comprising a non-metallic dopant element.

FIG. 9 shows non-metallic dopant element of Si concentration for as-deposited room temperature BiSbSi alloys vs. BiSbSi grain size as measured by inplane XRD patterns taken at 1 deg incident angle of various Si dopant element concentrations.

FIG. 10 shows the surface roughness of BiSbE alloy layers as determined by XRR as a function of atomic percent content of non-metallic dopant element of Si.

FIG. 11 shows the BiSbE alloy estimated grain size vs. estimated thickness for BiSbE for a non-metallic dopant element and for metallic dopant elements.

FIG. 12 is a plot of the logarithm of the intensity versus 2-theta XRD out-of-the plane or coupled scans of BiSbE stacks.

FIG. 13A is a schematic cross-sectional view of certain embodiments of a SOT device having a BiSbE alloy layer with (012) orientation forming a SOT-based magnetoresistive random access memory (MRAM) device.

FIG. 13B is a schematic cross-sectional view of certain embodiments of a SOT device having a BiSbE alloy layer with (012) orientation forming a portion or component of a SOT-based energy-assisted magnetic recording (EAMR) write head used in magnetic recording.

[0011] To facilitate understanding, identical reference numerals have been used, where possible, to designate identical elements that are common to the figures. It is contemplated that elements disclosed in one example may be beneficially utilized on other examples without specific recitation.

DETAILED DESCRIPTION

[0012] In the following, reference is made to embodiments of the invention and examples. However, it should be understood that the invention is not limited to specific Thus, the following aspects, features, embodiments and advantages are merely illustrative and are not considered elements or limitations of the appended claims except where explicitly recited in a claim(s). Likewise, a reference to "the disclosure" shall not be construed as a generalization of any inventive subject matter disclosed herein and shall not be considered to be an element or limitation of the appended claims except where explicitly recited in a claim(s). Usage in the Summary of the invention or in the Detailed Description of the term "comprising" shall mean comprising, consisting essentially, and/or consisting of.

[0013] Embodiments of the present invention generally relate to bismuth antimony (BiSb) alloys with (012) orientation for use as topological insulators as defined by the subject matter of the claims. The BiSb alloys comprise bismuth, antimony, and a dopant element (E) and are herein referred to as BiSbE alloys. The dopant element comprises a non-metallic dopant element, a metallic dopant element, or combinations thereof.

[0014] BiSbE alloy layers with (012) orientation have a large spin Hall angle effect and high electrical conductivity. Certain embodiments of the BiSbE alloy layers have reduced grain size and lower interfacial roughness in comparison to a BiSb material without dopant elements. Certain embodiments of the BiSbE alloy layers comprising a metallic dopant element have an increased melting temperature and allow higher annealing temperatures to be used while maintaining high (012) texture in comparison to a BiSb material without dopant elements. BiSbE alloy layers having (012) orientation can be used to form spin-orbit torque (SOT) devices, such as spin Hall electrode layers in MRAM devices or in an EAMR write heads. For example, BiSbE alloy layers are implemented into the manufacturing of SOT devices which are annealed to set magnetic directions of perpendicular magnetic anisotropy (PMA) ferromagnetic layers.

[0015] A prior BiSb layer with (012) orientation has a large spin Hall angle effect and high electrical conductivity. TABLE 1 shows one example of the properties of a BiSb layer with (012) orientation in comparison to beta-tantalum and to a BiSb layer with (001) orientation. A BiSb layer with (012) orientation has similar electrical conductivity and a much larger spin

Hall angle than beta-tantalum (Beta-Ta) or a BiSb layer with (001) orientation. Therefore, the relative power required to produce a spin Hall effect is lower for BiSb (012) in comparison to Beta-Ta or BiSb (001).

TABLE 1

	Spin Hall angle θ_{SH}	conductivity σ (10^6 $\Omega^{-1}m^{-1}$)	Power (relative)
Beta-Ta	-0.15	0.52	1
BiSb (001)	11	0.25	3.9×10^{-04}
BiSb (012)	52	0.25	1.7×10^{-05}

Prior BiSb materials with Sb content from about 5 atomic % to about 22 atomic % have melting points from about 270°C to about 300°C depending on the Sb content. During annealing, prior BiSb materials experience high levels of undesirable Sb migration due to the high roughness of the BiSb materials.

[0016] The present BiSbE alloy layers according to various embodiments disclosed herein have a high degree of (012) orientation, a large spin Hall angle effect, a low interfacial roughness, and a high electrical conductivity comparable to BiSb (012) materials without dopant elements. In certain embodiments, the BiSbE alloy layers with metallic dopant elements provide higher annealing temperatures to be used in comparison to BiSb materials without dopant elements.

[0017] In certain embodiments, a BiSbE alloy layer includes a non-metallic dopant element comprising Si, P, Ge, other suitable non-metallic dopant elements, or combinations thereof. In certain embodiments, a BiSbE alloy layer includes a metallic dopant element comprising Ni, Co, Fe, CoFe, NiFe, NiCo, NiCu, CoCu, NiAg, CuAg, Cu, Al, Zn, Ag, Ga, In, other suitable metallic dopant elements, or combinations thereof.

[0018] In certain embodiments, a BiSbE alloy layer comprises $Bi_{1-x}Sb_xE$ wherein x is $0.05 < x < 0.22$ and comprises the dopant element (E) from about 0.5 atomic % to about 15 atomic %.

[0019] Without being bound by theory unless specifically set forth in the claims, it is believed that the dopant element of the BiSbE alloy layer has a low solubility inside the BiSb lattice while maintaining the topological insulator property and the (012) orientation of the BiSb material. It is believed that a portion of the dopant element goes into the BiSb lattice after deposition. For example, in certain embodiments for a dopant element deposited at room temperature, a portion of the dopant element goes into the BiSb lattice and contracts the a-axis by about 0.5% and expands the c-axis from about 0.5 to about 1.0%. It is believed that a portion of the dopant element can act as a grain boundary segregant refining the structure of the BiSb grains or go to the BiSbE interfacial regions forming part of a seed layer or part of a cap layer.

[0020] FIG. 1A is a schematic illustration of a top down planar view of a BiSbE alloy layer 100 at deposition. The BiSbE alloy layer 100 comprises a plurality of BiSb lamellae layers 110 and one or more dopant element lamellae layers at deposition. The BiSbE alloy layer 100 comprises grains of BiSb and a layer of atoms/clusters 120 of dopant element(s) deposited uniformly over the grains of BiSb. It is believed that the atoms/clusters 120 of dopant element lamella layer forms uniformly over the BiSb lamella layer 110.

[0021] FIG. 1B is a schematic illustration of a top down planar view of the BiSbE alloy layer 100 after post annealing. It is believed that the atoms/clusters 120 of dopant element(s) have been redistributed to the grain boundaries of the BiSbE lamella layer 110. Some portion of the atoms/clusters 120 of dopant element is retained in the BiSb lattice while another portion of the atoms/clusters 120 of dopant element goes to the grain boundaries of the BiSb and to the BiSbE interfaces. The portion of the dopant element that goes to the grain boundaries of the BiSb becomes a segregant which reduces the grain size of the BiSb and reduces the interfacial roughness of the BiSbE alloy layer 100. In certain embodiments, the portion of the dopant element comprising metallic dopant elements that is retained in the BiSb lattice increases the melting point of the BiSbE alloy layer in comparison to a BiSb layer without dopant elements. The portion of the dopant element that is retained in the BiSb lattice allows the annealing temperature of the BiSbE alloy layer to be increased due to alloying (lattice hardening) and grain boundary segregation (grain size hardening) effects which pin and restrict the grain boundaries from moving at elevated temperatures. The BiSbE alloy layer is able to withstand an anneal, such as an anneal of about 280°C or above for three hours or more.

[0022] FIG. 1C is a schematic illustration of a cross-sectional layer view of the BiSbE alloy layer 100 after post annealing. It is believed that the atoms/clusters 120 of dopant element(s) have been redistributed to the grain boundaries of the BiSbE lamella layer 110 and to seed or cap layer interfaces, such as a silicide seed or silicide cap layer interfaces. The portion of the dopant element that goes to the grain boundaries becomes the segregant which reduces or modifies the grain size and lattice parameters of the grains 110 of BiSb and reduces the interfacial roughness of the BiSbE alloy layer 100.

[0023] In certain embodiments, the interfacial roughness of the BiSbE alloy layer with a silicide seed layer and with a silicide cap layer is about 14 Å or less. In certain embodiments, interfacial roughness of the BiSbE alloy layer with a silicide seed layer and a silicide cap layer is reduced by about from about 3 Å to about 5 Å in comparison to a BiSb material without dopant elements. The use of a metal interlayers between the BiSbE alloy layer and the silicide seed layer and between the

BiSbE alloy layer and the silicide cap layer further reduces the interfacial roughness for the BiSbE alloy layer.

[0024] The (012) texture is enhanced with a BiSbE alloy layer in comparison to a BiSb without dopant elements. For example, in certain embodiments, the (012) texture of a BiSbE alloy stack of a silicide seed layer, a metal interlayer, a BiSbE alloy layer, a metal interlayer, a silicide cap layer has a rocking curve with widths less than 11 degrees, such as from about 7 to about 10 degrees. In comparison, the (012) texture of a BiSb stack without dopant elements of a stack of a silicide seed layer, a metal interlayer, a BiSb layer, a metal interlayer, a silicide cap layer has a rocking curve with widths of about 10 degrees or more and with a dual (001) and (012) texture.

[0025] In certain embodiments, the BiSbE alloy layer is formed to a thickness from about 20 Å to about 200 Å, such as from about 50 Å to about 150 Å. In other embodiments, the BiSbE alloy layer is formed to any suitable thickness. In certain embodiments, the BiSbE alloy layer is deposited by physical vapor deposition (PVD), such as sputtering, molecular beam epitaxy, ion beam deposition, other suitable PVD processes, and combinations thereof. In certain embodiments, a SOT device includes a BiSbE alloy layer formed over any suitable layer and with any suitable layer formed over the BiSbE alloy layer.

[0026] In embodiments, the BiSbE alloy layer comprises a multi-layer laminate of a plurality of BiSb lamellae layers and one or more dopant element lamellae layers. The BiSbE alloy multi-layer laminate provides placement of the dopant element lamella layer at specific regions of the BiSbE alloy layer to increase nucleation and growth of (012) orientation, to reduce interfacial roughness, and/or to reduce grain size.

[0027] In one embodiment, the BiSbE alloy layer comprises 2 to 10 BiSb lamellae layers with each BiSb lamella layer having a thickness from about 5 Å to about 30 Å and comprises 1 to 9 dopant element lamellae layers with each dopant element lamella layer having a thickness from about 0.1 Å to about 4 Å. One or more dopant element lamellae layers are interspersed between the BiSb lamellae layers. In other embodiments, the BiSbE alloy layer comprises any suitable number of BiSb lamellae layers with each BiSb lamella layer formed to any suitable thickness and comprises any suitable number of dopant element lamellae layers with each dopant element lamella layer formed to any suitable thickness.

[0028] FIG. 2A is a schematic illustration of deposition of a BiSbE alloy layer 200 comprising six BiSb lamellae layers 210 and five dopant element lamellae layers 220. A dopant element lamella layer 220 has been deposited between each of the BiSb lamellae layers 210. The dopant element lamellae layers 220 have been deposited throughout the BiSbE alloy layer 200. FIG. 2B is a schematic illustration of the distribution of the dopant element within the BiSb lamellae layers 210 of the BiSbE alloy layer 200 at deposition or after annealing. The dopant element is distributed into each of the BiSb lamellae layers 210.

[0029] FIG. 2C is a schematic illustration of deposition of a BiSbE alloy layer 200 comprising six BiSb lamellae layers 210 and four dopant element lamellae layers 220. The BiSbE alloy layer 200 can also be viewed as two thin BiSb lamellae layers 210 at the bottom edge, two thin BiSb lamellae layers 210 at the top edge, and a thick BiSb lamella layer 210T at the center with dopant element lamellae layers 220 therebetween. The dopant element lamellae layers 220 have been deposited at the bottom edge and the top edge of the BiSbE alloy layer 200 but not at the center of the BiSbE alloy layer 200. FIG. 2D is a schematic illustration of the distribution of the dopant element within the BiSb lamellae layers 210 of the BiSbE alloy layer 200 at deposition or after annealing. The dopant element is distributed at the bottom edge and the top edge of the BiSbE alloy layer 200.

[0030] FIG. 2E is a schematic illustration of deposition of a BiSbE alloy layer 200 comprising six BiSb lamellae layers 210 and three dopant element lamellae layers 220. The BiSbE alloy layer 200 can also be viewed as one thin BiSb lamella layer 210 at the bottom edge, one thin BiSb lamella layer 210 at the top edge, and two thick BiSb lamellae layers 210T at the center with dopant element lamellae layers 220 therebetween. The dopant element lamellae layers 220 have been deposited every other BiSb lamella layer 210. The dopant element lamellae layers 220 have been deposited at the bottom edge, the center, and the top edge of the BiSbE alloy layer 200. FIG. 2F is a schematic illustration of the distribution of the dopant element within the BiSb lamellae layers 210 of the BiSbE alloy layer 200 at deposition or after annealing. The dopant element is distributed at the bottom edge, the center, and the top edge of the BiSbE alloy layer 200.

[0031] FIG. 2G is a schematic illustration of deposition of a BiSbE alloy layer 200 comprising six BiSb lamellae layers 210 and three dopant element lamellae layers 220. The BiSbE alloy layer 200 can be viewed as three thin BiSb lamellae layers 210 at the bottom edge and one thick BiSb lamella layer 210T at top edge with dopant element lamellae layers 220 therebetween. The dopant element lamellae layers 220 have been deposited at the bottom edge but not at the top edge of the BiSbE alloy layer 200. FIG. 2H is a schematic illustration of the distribution of the dopant element within the BiSb lamellae layers 210 of the BiSbE alloy layer 200 at deposition or after annealing. The dopant element is distributed at the bottom edge of the BiSbE alloy layer 200.

[0032] FIG. 13A is a schematic cross-sectional view of certain embodiments of a SOT device 10 having a BiSbE alloy layer 50 with (012) orientation forming a SOT-based magnetoresistive random access memory (MRAM) device as defined by the subject matter of the claims.

[0033] The BiSbE alloy layer 50 with (012) orientation is formed over a substrate 20, such as a silicon substrate, an alumina substrate, or other suitable substrates. A seed layer 30 is deposited over the substrate 20. The seed layer 30 comprises a silicide layer 32 or other suitable seed layers. In certain embodiments, the silicide layer 32 comprises NiSi,

NiFeSi, NiFeTaSi, NiCuSi, CoSi, CoFeSi, CoFeTaSi, CoCuSi, or combinations thereof. In certain embodiments, the seed layer 30 further comprises a surface control layer 40 between the silicide layer 32 and the BiSbE alloy layer 50. In certain embodiments, the surface control layer 40 comprises NiFe, NiFeTa, NiTa, NiW, NiFeW, NiCu, NiFeCu, CoTa, CoFeTa, NiCoTa, Co, CoM, CoNiM, CoNi, NiSi, CoSi, NiCoSi, Cu, CuAg, CuAgM, CuM, or combinations thereof, in which M is Fe, Cu, Co, Ta, Ag, Ni, Mn, Cr, V, Ti, or Si.

[0034] In certain embodiments, an interlayer 70 is deposited over the BiSbE alloy layer 50. The interlayer 70 comprises a silicide layer 72. In certain embodiments, the silicide layer 72 comprises NiSi, FeSi, CoSi, NiCuSi, NiFeTaSi, CoFeSi, CoCuSi, or combinations thereof. In certain embodiments, the interlayer 70 further comprises a surface control layer 71 between the BiSbE alloy layer 50 and the silicide layer 72. The surface control layer 71 comprises Cu, Ni, NiFe, Co, or combinations thereof.

[0035] A free perpendicular magnetic anisotropy (PMA) layer 80 is formed over the interlayer 70. For example, the free PMA layer 80 can comprise one or more stacks of a Co/Pt, Co/Pd, Co/Ni, CoFeB, FePt or other PMA inducing layers or combinations thereof. An insulating layer 84, such as a MgO layer, is formed over the free PMA layer 80. A reference PMA layer 88 is formed over the insulating layer 84. The reference PMA layer 88 can comprise one or more stacks of a Co/Pt, Co/Pd, Co/Ni, CoFeB, FePt or other PMA inducing layers or combinations thereof. The reference PMA layer 88 can include one or more synthetic antiferromagnetic (SAF) pinned structures. A cap layer 92 can be formed over the reference PMA layer 88. The cap layer 92 comprises NiFe, SiN, Si, NiFeTa, NiTa, Pt, Co, Cu, Ni, NiCu, CoCu, Ru, Ta, Cr, Au, Rh, CoFe, CoFeB, other non-magnetic materials, other magnetic materials, and combinations thereof. The magnetic direction of the reference PMA layer 88 can be set with an anneal of about 270°C or above for two hours or more. In certain embodiment, the BiSbE alloy layer 50 comprises a metallic dopant element. The metallic dopant element of the BiSbE alloy layer 50 helps to maintain the low interfacial roughness of the BiSbE alloy layer 50 after anneal and helps to the manufacturability, performance, and/or life time of the MRAM device. The BiSbE alloy layer 50 comprises a metallic dopant element has reduced migration of Sb of the BiSbE alloy layer 50 after post annealing in comparison to a BiSb material without dopant elements.

[0036] A plurality of the SOT devices 10 can be configured together as part of a memory cell array in which the BiSbE alloy layer 50 is a spin orbit material electrode. A top electrode (not shown) can be disposed over the reference PMA layer 88. Each of the memory cells may be part of a two-terminal device or a three terminal device. The spin orbit material electrode and the top electrode may serve as bit lines, word lines, read word lines, write word lines, and combinations thereof. The memory cell array may be implemented as a crosspoint array or other architectures.

[0037] FIG. 13B is a schematic cross-sectional view of certain embodiments of a SOT device 10 having a BiSbE alloy layer 50 with (012) orientation forming a portion or component of a SOT-based EAMR write head used in magnetic recording as defined by the subject matter of the claims.

[0038] The BiSbE alloy layer 50 with (012) orientation is formed over a substrate 20, such as a silicon substrate, an alumina substrate, or other suitable substrates. A seed layer 30 is deposited over the substrate 20. The seed layer 30 comprises a silicide layer 32 or other suitable seed layers. In certain embodiments, the silicide layer 32 comprises NiSi, NiFeSi, NiFeTaSi, NiCuSi, CoSi, CoFeSi, CoFeTaSi, CoCuSi, or combinations thereof. In certain embodiments, the seed layer 30 further comprises a surface control layer 40 between the silicide layer 32 and the BiSbE alloy layer 50. In certain embodiments, the surface control layer 40 comprises NiFe, NiFeTa, NiTa, NiW, NiFeW, NiCu, NiFeCu, CoTa, CoFeTa, NiCoTa, Co, CoM, CoNiM, CoNi, NiSi, CoSi, NiCoSi, Cu, CuAg, CuAgM, CuM, or combinations thereof, in which M is Fe, Cu, Co, Ta, Ag, Ni, Mn, Cr, V, Ti, or Si.

[0039] In certain embodiments, an interlayer 70 is deposited over the BiSbE alloy layer 50. The interlayer 70 comprises a silicide layer 72. In certain embodiments, the silicide layer 72 comprises NiSi, FeSi, CoSi, NiCuSi, NiFeTaSi, CoFeSi, CoCuSi, or combinations thereof. In certain embodiments, the interlayer 70 further comprises a surface control layer 71 between the BiSbE alloy layer 50 and the silicide layer 72. The surface control layer 71 comprises Cu, Ni, NiFe, Co, or combinations thereof.

[0040] A spin-torque layer (STL) 60 is formed over the interlayer 70. The STL 60 comprises a ferromagnetic material such as one or more layers of CoFe, CoIr, NiFe, and CoFeM wherein M = B, Ta, Re, or Ir. Charge current through a BiSbE alloy layer 50 acting as a spin Hall layer generates a spin current in the BiSbE layer 50. The spin-orbital coupling of the BiSbE alloy layer 50 and a spin torque layer (STL) 60 causes switching or precession of magnetization of the STL 60 by the spin-orbital coupling of the spin current from the BiSbE alloy layer 50. Switching or precession of the magnetization of the STL 60 can generate an assisting DC field to the write field from a main pole of a write head used in magnetic recording. SOT based EAMR elements have multiple times greater power efficiency in comparison to spin-transfer torque (STT) based Microwave-Assisted Magnetic Recording (MAMR) elements. In an embodiment, the BiSbE alloy layer 50 comprises a metallic dopant element or a non-metallic dopant element. For example, if the SOT-based EAMR write head is not annealed, a BiSbE alloy layer 50 comprising a non-metallic dopant element can be used since degradation of the interfacial roughness due to post annealing is avoided.

[0041] A SOT device includes a bismuth antimony dopant element (BiSbE) alloy layer over a substrate. The BiSbE alloy layer is used as a topological insulator, such as for SOT-based MRAM device or for SOT-based EAMR write head. The

BiSbE alloy layer includes bismuth, antimony, a dopant element. The dopant element can be a non-metallic dopant element comprising Si, P, Ge, or combinations thereof, a metallic dopant element comprising Ni, Co, Fe, CoFe, NiFe, Cu, Al, Zn, Ag, Ga, In, or combinations thereof, or a combination of a non-metallic dopant element(s) and a metallic dopant element(s). The BiSbE alloy layer can include a plurality of BiSb lamellae layers and one or more dopant element lamellae layers. The BiSbE alloy layer has a (012) orientation. In certain embodiments, the BiSbE alloy layer has a higher annealing temperature, stronger (012) texture, smaller grain size, and/or lower surface roughness in comparison to a BiSb material without dopant elements.

[0042] In one example, a SOT device includes a bismuth antimony dopant element (BiSbE) alloy layer over a substrate. The BiSbE alloy layer includes bismuth, antimony, and a dopant element. The dopant element is a non-metallic dopant element, a metallic dopant element, and combinations thereof. Examples of metallic dopant elements include Ni, Co, Fe, CoFe, NiFe, NiCo, NiCu, CoCu, NiAg, CuAg, Cu, Al, Zn, Ag, Ga, In, or combinations thereof. Examples of non-metallic dopant elements include Si, P, Ge, or combinations thereof. The BiSbE alloy layer has a (012) orientation.

[0043] In another example, a SOT device includes a bismuth antimony dopant element (BiSbE) alloy layer over a substrate. The BiSbE alloy layer includes a plurality of BiSb lamellae layers and one or more dopant element lamellae layers. Each of the dopant element lamellae layers includes a non-metallic dopant element, a metallic dopant element, and combinations thereof. Examples of metallic dopant elements include Ni, Co, Fe, CoFe, NiFe, NiCo, NiCu, CoCu, NiAg, CuAg, Cu, Al, Zn, Ag, Ga, In, or combinations thereof. Examples of non-metallic dopant elements include Si, P, Ge, or combinations thereof. The BiSbE alloy layer has a (012) orientation.

[0044] In still another example, a magnetoresistive random access memory (MRAM) device includes a bismuth antimony dopant element (BiSbE) alloy layer. The BiSbE alloy layer includes bismuth, antimony, and a metallic dopant element. The metallic dopant element is Ni, Co, Fe, CoFe, NiFe, NiCo, NiCu, CoCu, NiAg, CuAg, Cu, Al, Zn, Ag, Ga, In, or combinations thereof. The BiSbE alloy layer having a (012) orientation. The MRAM device further includes a perpendicular magnetic anisotropy (PMA) ferromagnetic layer.

EXAMPLES

[0045] The following are examples to illustrate various embodiments of a BiSbE alloy layer 50, 100, 200 of FIGS. 1, 2A-2H, or 13A-13B, other SOT devices, and variations thereof. These examples are not meant to limit the scope of the claims unless specifically recited in the claims.

Example 1

[0046] FIG. 3 shows 2-theta XRD scans vs. logarithm of the intensity of the BiSb orientation of various stacks 310-360 of BiSbE alloy layers comprising a non-metallic dopant element of Si. Each of the stacks 310-360 comprised a seed layer of a NiFeCu-silicide layer formed to a thickness of about 18 Å and a copper alloy (CuAgNi) layer formed to a thickness of about 1 Å, a BiSbE alloy layer formed to a thickness of about 100 Å, an interlayer of a NiFe-silicide layer formed to a thickness of about 14 Å, and a cap layer of SiN formed to a thickness of 60 Å. The BiSbSi alloy layers comprised a plurality of BiSb lamellae layers and a plurality of Si lamellae layers in which the dopant element comprised Si. Each of the BiSb lamellae layers comprised about 90 atomic % of Bi and about 10 atomic % of Sb.

[0047] The BiSbE alloy layer of stack 310 was formed by depositing six BiSb lamellae layers with each BiSb lamella layer deposited to a thickness of about 15 Å and by depositing three Si lamellae layers with each Si lamella layer deposited to a thickness of about 0.5 Å. The Si lamellae layers were deposited at the top edge of the BiSbE alloy layer in the order of BiSb-BiSb-BiSb-Si-BiSb-Si-BiSb-Si-BiSb (BBBSBSBSB).

[0048] The BiSbE alloy layer of stack 320 was formed by depositing six BiSb lamellae layers with each BiSb lamella layer deposited to a thickness of about 15 Å and by depositing three Si lamellae layers with each Si lamella layer deposited to a thickness of about 0.5 Å. The Si lamellae layers were deposited at the center of the BiSbE alloy layer in the order of BiSb-BiSb-Si-BiSb-Si-BiSb-Si-BiSb-BiSb (BBSBSBSBB).

[0049] The BiSbE alloy layer of stack 330 was formed by depositing six BiSb lamellae layers with each BiSb lamella layer deposited to a thickness of about 15 Å and by depositing three Si lamellae layers with each Si lamella layer deposited to a thickness of about 0.5 Å. The Si lamellae layers were deposited at the bottom edge of the BiSbE alloy layer in the order of BiSb-Si-BiSb-Si-BiSb-Si-BiSb-BiSb-BiSb (BSBSBSBBB).

[0050] The BiSbE alloy layer of stack 340 was formed by depositing six BiSb lamellae layers with each BiSb lamella layer deposited to a thickness of about 15 Å and by depositing three Si lamellae layers with each Si lamella layer deposited to a thickness of about 0.5 Å. The Si lamellae layers were modulated within the BiSbE alloy layer in the order of BiSb-Si-BiSb-BiSb-Si-BiSb-BiSb-Si-BiSb (BSBBSBBSB).

[0051] The BiSbE alloy layer of stack 350 was formed by depositing six BiSb lamellae layers with each BiSb lamella layer deposited to a thickness of about 15 Å and by depositing four Si lamellae layers with each Si lamella layer deposited to a thickness of about 0.5 Å. The Si lamellae layers were deposited at the bottom edge and the top edge of the BiSbE alloy

layer in the order of BiSb-Si-BiSb-Si-BiSb-BiSb-Si-BiSb-Si-BiSb (BSBSBBSBSB).

[0052] The BiSbE alloy layer of stack 360 was formed by depositing six BiSb lamellae layers with each BiSb lamella layer deposited to a thickness of about 15 Å and by depositing five Si lamellae layers with each Si lamella layer deposited to a thickness of about 0.5 Å. The Si lamellae layers were deposited throughout the BiSbE alloy layer in the order of BiSb-Si-BiSb-Si-BiSb-Si-BiSb-Si-BiSb (BSBSBSBSBSB).

[0053] Stack 310 with a top edge distribution of the dopant element Si and stack 320 with a center distribution of dopant element Si do not promote strong BiSbSi (012) orientation. Stack 330 with a bottom edge distribution of dopant element Si, stack 340 with a modulated distribution of dopant element Si, stack 350 with a bottom edge and top edge distribution of dopant element Si, and stack 360 with a dopant element Si distribution the throughout the BiSbE alloy layer promoted strong BiSbSi(012) orientation.

Example 2

[0054] FIG. 4 shows 2-theta XRD scans vs. logarithm of the intensity of the BiSb orientation of various stacks 410-460 of BiSbE alloy layers comprising a metallic dopant element of CuAgNi. The BiSbE alloy layers comprised a plurality of BiSb lamellae layers and a plurality of lamellae layers of metallic dopant element of CuAgNi. Each of the BiSb lamellae layers comprised about 90 atomic % of Bi and about 10 atomic % of Sb. Each of the stacks 410-460 comprised a seed layer of a NiFeCu-silicide layer formed to a thickness of about 18 Å, a BiSbE alloy layer formed to a thickness of about 100Å, an interlayer of a NiFe-silicide layer formed to a thickness of about 14 Å, and a cap layer of SiN formed to a thickness of 60 Å.

[0055] The BiSbE alloy layer of stack 410 was formed by depositing six BiSb lamellae layers with each BiSb lamella layer deposited to a thickness of about 15 Å and by depositing three CuAgNi lamellae layers with each CuAgNi lamella layer deposited to a thickness of about 0.5 Å. The CuAgNi lamellae layers were deposited at the top edge of the BiSbE alloy layer in the order of BiSb-BiSb-BiSb-CuAgNi-BiSb-CuAgNi-BiSb-CuAgNi-BiSb (BBBCBCBB).

[0056] The BiSbE alloy layer of stack 420 was formed by depositing six BiSb lamellae layers with each BiSb lamella layer deposited to a thickness of about 15 Å and by depositing three CuAgNi lamellae layers with each CuAgNi lamella layer deposited to a thickness of about 0.5 Å. The CuAgNi lamellae layers were deposited at the center of the BiSbE alloy layer in the order of BiSb-BiSb-CuAgNi -BiSb-CuAgNi-BiSb-CuAgNi-BiSb-BiSb (BBCBCBCBB).

[0057] The BiSbE alloy layer of stack 430 was formed by depositing six BiSb lamellae layers with each BiSb lamella layer deposited to a thickness of about 15 Å and by depositing three CuAgNi lamellae layers with each CuAgNi lamella layer deposited to a thickness of about 0.5 Å. The CuAgNi lamellae layers were deposited at the bottom edge of the BiSbE alloy layer in the order of BiSb-CuAgNi -BiSb-CuAgNi-BiSb-CuAgNi-BiSb-BiSb-BiSb (BCBCBCBBB).

[0058] The BiSbE alloy layer of stack 440 was formed by depositing six BiSb lamellae layers with each BiSb lamella layer deposited to a thickness of about 15 Å and by depositing three CuAgNi lamellae layers with each CuAgNi lamella layer deposited to a thickness of about 0.5 Å. The CuAgNi lamellae layers were modulated within the BiSbE alloy layer in the order of BiSb-CuAgNi-BiSb-BiSb-CuAgNi-BiSb-BiSb-CuAgNi-BiSb (BCBBCBBCB).

[0059] The BiSbE alloy layer of stack 450 was formed by depositing six BiSb lamellae layers with each BiSb lamella layer deposited to a thickness of about 15 Å and by depositing four CuAgNi lamellae layers with each CuAgNi lamella layer deposited to a thickness of about 0.5 Å. The CuAgNi lamellae layers were deposited at the bottom edge and the top edge of the BiSbE alloy layer in the order of BiSb-CuAgNi-BiSb-CuAgNi-BiSb-BiSb-CuAgNi-BiSb-CuAgNi-BiSb (BCBCBB-CBCB).

[0060] The BiSbE alloy layer of stack 460 was formed by depositing six BiSb lamellae layers with each BiSb lamella layer deposited to a thickness of about 15 Å and by depositing five CuAgNi lamellae layers with each CuAgNi lamella layer deposited to a thickness of about 0.5 Å. The CuAgNi lamellae layers were deposited throughout the BiSbE alloy layer in the order of BiSb-CuAgNi-BiSb-CuAgNi-BiSb-CuAgNi-BiSb-CuAgNi-BiSb-CuAgNi-BiSb (BCBCBCBCBCB).

[0061] Stack 410 with a top edge distribution of the CuAgNi, stack 420 with a center distribution of CuAgNi, and stack 440 with a modulated distribution of CuAgNi do not promote strong BiSbE (012) orientation. Stack 430 with a bottom edge distribution of CuAgNi, stack 450 with a bottom edge and top edge distribution of CuAgNi, and stack 460 with a CuAgNi distribution throughout the BiSbE alloy layer promoted strong BiSbE(012) orientation.

Example 3

[0062] FIG. 5 shows a plot of the TOF-SIMS net Intensity for dopant E-Cs+ clusters across the BiSbE alloy layer for dopant elements of NiFe, Si, and CuAgNi as a function of sputter time in seconds. BiSbE sample 510 with atomic percent content of a dopant element of silicon of about 17%, a BiSbE sample 520 with atomic percent content of a dopant element of CuAgNi of about 14%, a BiSbE sample 530 with atomic percent content of a dopant element of NiFe of about 14%. BiSbE sample 510 was formed with a modulated distribution of Si dopant element. BiSbE sample 520 was formed with an edge distribution of CuAgNi dopant element. BiSbE sample 530 was formed with an edge distribution of NiFe dopant element. The net intensity is the absolute intensity of the E-Cs+ cluster of BiSbE minus the intensity of E-Cs+ cluster of a BiSbE

which contains no dopant element. Each of the samples 510-530 included a NiFeCu silicide seed layer of about 16 Å, about 1 Å of Cu, about 7 Å of NiFe, about 1 Å of Cu, and a NiFeCu silicide cap layer of about 2 Å of Cu, 16 Å of Si, and 8 Å of NiFe. The locations of the centers of the NiFeCu silicide seed layer, the NiFeCu silicide cap layer, and the BiSbE alloy layer are indicated with vertical black dashed lines.

[0063] FIG. 5 shows a portion of the dopant elements are pushed out of the BiSbE alloy layer. FIG. 5 shows a non-zero net TOF-SIMS intensity inside the BiSbE alloy layer indicating a portion of the dopant elements remain in the BiSbE lattice after deposition.

Example 4

[0064] FIG. 6 shows TEM Cu EELS scans across a BiSbE stack comprising a silicide cap layer, a BiSbE alloy layer comprising a metallic dopant of CuAgNi, and a silicide seed layer. The BiSbE alloy layer comprised a metallic dopant of CuAgNi in an atomic percent content of about 6%. The metallic dopant of CuAgNi comprised Ag in an atomic percent content of about 5% and with Ni in an atomic percent content of about 10%. The BiSbE stack included a NiFeCu silicide seed layer of about 20 Å, about 1 Å of Cu, a BiSbE alloy layer of about 100 Å, a NiFeCu silicide cap layer of about 30 Å, and a SiN layer of about 60 Å.

[0065] The BiSbE alloy layer comprised the metallic dopant element in the center of the BiSbE alloy layer going higher towards the interfaces for both room temperature and after post annealing at about 280°C for 3 hours. A portion of the CuAgNi dopant element is leaving BiSb lattice and a portion of the CuAgNi dopant element is retained in the BiSb lattice even after the post annealing near the melting point of the BiSbE alloy layer.

[0066] A portion of the dopant element has been retained in the lattice after near melting. It is believed that on anneal the BiSbE lattice relaxed the lattice parameters with a portion of the dopant elements residing within the BiSbE lattice forming the alloy and with a portion diffusing to the interlayer interfaces or to the grain boundaries.

Example 5

[0067] FIG. 7 shows the as deposited conductivity versus thickness of BiSbE alloy layers 710-750 comprising a metallic dopant as measured by XRR/XRF. Each of the BiSbE alloy layers 710-750 were formed over a Si seed layer having a thickness of about 30 Å. Conductivity (1/Resistance) was measured using a four-point probe. The fitted curves assume a 2-resistor model of a surface conductive layer and a bulk conductive layer and fit an 'A + B/thickness' model.

[0068] BiSb layer 740 is a layer of pure BiSb without dopant elements, BiSbE alloy layer 710 comprised BiSbCu with an atomic percent content of Cu of about 10%. BiSbE alloy layer 720 comprised BiSbCu with an atomic percent content of Cu of about 14%. BiSbE alloy layer 730 comprised BiSbCu with an atomic percent content of Cu of about 20%. BiSbE alloy layer 750 comprised BiSb-NiFe with an atomic percent content of NiFe of about 10%.

[0069] BiSbE alloy layers 720, 710, 750 showed good topological insulator properties similar to reference BiSb layer 740. BiSbE alloy layer 730 showed bulk conduction rather than topological insulator properties.

Example 6

[0070] FIG. 8 shows the as deposited conductivity versus thickness of various BiSbE alloy layers 820-860 comprising a non-metallic dopant elements of Si as measured by XRR/XRF. Each of the BiSbE alloy layers 820-860 were measured for thickness by XRR and were formed over a Si seed layer having a thickness of about 30 Å. Conductivity (1/Resistance) was measured using a four-point probe. The fitted curves assume a 2-resistor model of a surface conductive layer and a bulk conductive layer and fit an 'A + B/thickness' model.

[0071] BiSb alloy layer 810 comprised BiSb as a reference layer. BiSbE alloy layer 820 comprised BiSbSi with an atomic percent content of Si of about 4%. BiSbE alloy layer 830 comprised BiSbSi with an atomic percent content of Si of about 5%. BiSbE alloy layer 840 comprised BiSbSi with an atomic percent content of Si of about 9%. BiSbE alloy layer 850 comprised BiSbSi with an atomic percent content of Si of about 13%. BiSbE alloy layer 860 comprised BiSbSi with an atomic percent content of Si of about 15%.

[0072] BiSbE alloy layers 820-860 showed good topological insulator properties similar to BiSb reference layer 810 after deposition. BiSbE alloys layers comprising BiSbSi having an atomic percent content of Si from 0% to about 15% showed good topological insulator properties.

Example 7

[0073] FIG. 9 shows Si dopant element concentration for BiSbSi alloys vs. BiSbSi grain sizes as measured by inplane XRD patterns taken at 1 deg incident angle of various BiSbSi alloy layers. Each of the BiSbSi alloy layers were formed over a-Si seed layer having a thickness of about 30 Å and with a Si cap layer formed over the BiSbSi alloy layer having a

thickness of about 30 Å. The BiSbSi alloy layers showed a large reduction trend in grain size as the atomic percent of Si is increased from 0% to about 10%. The BiSbSi alloy layers showed a small reduction trend in grain size as the atomic percent of Si is increased from more than about 10%. Although the grain size of a BiSbSi alloy with an about 10 atomic % content of Si is much reduced in comparison to a BiSb material without dopant elements, further increasing the atomic percent content of Si above 10% produces only a small additional reduction in the grain size.

Example 8

[0074] FIG. 10 shows the surface roughness of BiSbE alloy layers 610, 620 as determined by XRR as a function of atomic percent content of non-metallic dopant element of Si.

[0075] Each of the BiSbE alloy layers were formed over a Si seed layer having a thickness of about 30 Å and a Si capping layer formed thereover having a thickness of about 30 Å. Each of the BiSbE alloy layers were deposited to a thickness of about 100 Å. BiSbE alloy layer 610 comprised BiSbSi with varying atomic percent content of silicon. BiSbE alloy layer 620 comprised BiSbCu with varying atomic percent content of copper.

[0076] FIG. 10 shows that the dopant elements reduced interface roughness in comparison to a BiSb layer without dopant elements. The BiSbE alloy layer with an atomic percent content of the dopant element from about 3% to about 12% produced a large reduction in surface roughness in comparison to a BiSb material without dopant elements. The BiSbE alloy layer with an atomic percent content of the dopant element greater than 12% were comparable to a BiSb material without dopant elements with larger interfacial roughness.

Example 9

[0077] FIG. 11 shows the BiSbE alloy estimated grain size from in plane XRD patterns taken at approximately 1 deg. incident angle vs. estimated thickness for BiSbE by XRR for a non-metallic dopant element of Si, a metallic dopant element of Cu, a metallic dopant element of NiFe compared to BiSb without dopant elements. Estimated dopant element concentrations deposited into the film are given in the plot. BiSb layer 1110 comprised BiSb without dopant elements. BiSbE alloy layer 1120 comprised a dopant element Si in an atomic percent content of about 5%. BiSbE alloy layer 1130 comprised dopant element Cu in an atomic percent content of about 10%. BiSbE alloy layer 1140 comprised dopant element Cu in an atomic percent content of about Cu6% which was annealed at about 280°C for 3 hours. BiSbE alloy layer 1150 comprised dopant element NiFe in an atomic percent content of about 10%. Dopant elements reduce the grain size for all BiSbE alloy thicknesses.

Example 10

[0078] FIG. 12 is a plot of the logarithm of the intensity versus 2-theta XRD out-of-the plane or coupled scans of BiSbE stacks 1210, 1220. The BiSbE alloy layer comprised a metallic dopant of CuAgNi in an atomic percent content of about 6%. The metallic dopant of CuAgNi comprised Ag in an atomic percent content of about 5% and with Ni in an atomic percent content of about 10%. The BiSbE alloy layer was formed by depositing six BiSb lamellae layers and by depositing four CuAgNi lamellae layers. The CuAgNi lamellae layers were deposited at the bottom edge and the top edge of the BiSbE alloy layer in the order of BiSb-CuAgNi-BiSb- CuAgNi-BiSb-BiSb-CuAgNi-BiSb-CuAgNi-BiSb (BCBCBBCBCB).

[0079] Each of the stacks 1210, 1220 comprised a NiFeCu-silicide layer formed to a thickness of about 20 Å, a copper layer formed to a thickness of about 1 Å, a BiSbE alloy layer formed to a thickness of about 100 Å, an NiFeCu-silicide layer formed to a thickness of about 14 Å, and a capping layer of SiN formed to a thickness of about 60 Å. BiSbE stack 1210 was before annealing. BiSbE stack 1220 is after annealing at about 280°C for about 3 hours near the melting point of BiSb. BiSbE stacks 1210, 1220 showed strong (012) texture before and after annealing. The BiSbE stack 1220 showed strong (012) texture even after annealing near the melting point of BiSb with a rocking curve of about 11 degrees or less, such as from 7 degrees to 11 degrees. An XRR measurement of the BiSbE stack 1220 after anneal showed a low surface roughness of about 14 Å or less.

[0080] While the foregoing is directed to embodiments of the present invention and examples, other and further embodiments of the invention may be devised without departing from the invention as defined by the claims.

Claims

1. A spin-orbit torque, SOT, device (10), comprising:

a substrate (20); and
a bismuth antimony dopant element, BiSbE, alloy layer (50; 200) over the substrate, the BiSbE

alloy layer having a (012) orientation, the BiSbE alloy layer comprising,

bismuth;
antimony; and
a dopant element,

wherein the bismuth and antimony of the BiSbE alloy layer form a plurality of BiSb lamellae layers (210), wherein the dopant element of the BiSbE alloy layer forms one or more dopant element lamellae layers (220), each of the dopant element lamellae layers comprising a material selected from a group consisting of a non-metallic dopant element, a metallic dopant element, and combinations thereof, and
wherein the BiSbE alloy layer comprises the one or more dopant element lamellae layers at a bottom edge of the BiSbE alloy layer.

2. The SOT device of claim 1, wherein the metallic dopant element is selected from a group consisting Ni, Co, Fe, CoFe, NiFe, NiCo, NiCu, CoCu, NiAg, CuAg, Cu Al, Zn, Ag, Ga, In, and combinations thereof.

3. The SOT device of claim 1, wherein the non-metallic dopant element is selected from a group consisting Si, P, Ge, and combinations thereof.

4. The SOT device of claim 1, wherein the BiSbE alloy layer comprises the dopant element at a concentration from 0.5 atomic % to 15 atomic %.

5. The SOT device of claim 1, wherein the BiSbE alloy layer comprises $Bi_{1-x}Sb_xE$ wherein x is $0.05 < x < 0.22$.

6. The SOT device of claim 1, wherein the BiSbE alloy layer is formed to a thickness from 20 Å to 200 Å.

7. The SOT device of claim 1, wherein the BiSbE alloy layer further comprises the one or more dopant element lamellae layers at a top edge of the BiSbE alloy layer.

8. The SOT device of claim 1, wherein the dopant element of the BiSbE alloy layer forms a plurality of dopant element lamellae layers and wherein the BiSbE alloy layer further comprises the dopant element lamellae layers stacked in a modulated manner in the BiSbE alloy layer.

9. The SOT device of claim 1, wherein the BiSbE alloy layer further comprises the one or more dopant element lamellae layers throughout the BiSbE alloy layer.

10. A SOT-based energy-assisted magnetic recording, EAMR, write head, comprising the SOT device of claim 1, wherein the BiSbE alloy layer (50) is proximate to a spin-torque layer (60).

11. A magnetoresistive random access memory, MRAM, device, comprising the SOT device of claim 2, the SOT device further comprising at least one perpendicular magnetic anisotropy, PMA, ferromagnetic layer (80, 88).

12. The MRAM device of claim 11, wherein the BiSbE alloy layer (50) is a spin orbit material electrode proximate to a free PMA layer (80).

13. The MRAM device of claim 11, wherein the PMA ferromagnetic layer is a reference PMA ferromagnetic layer (88), the reference PMA ferromagnetic layer having a magnetic direction set by an anneal of 270°C or above for two hours or more.

14. The MRAM device of claim 13, wherein the BiSbE alloy layer (50) has a roughness, R_a, of 14 Å or less after the reference PMA ferromagnetic layer (88) is annealed.

15. The MRAM device of claim 11, wherein the BiSbE alloy layer (50) exhibits strong (012) texture and has a rocking curve of 11 degrees or less.

16. The MRAM device of claim 13, wherein the BiSbE alloy layer (50) is a topological insulator after the reference PMA ferromagnetic layer (88) is annealed.

Patentansprüche

1. Eine Vorrichtung (10) mit Spin-Orbit-Drehmoment, SOT, die Folgendes beinhaltet:

   ein Substrat (20); und
   eine Bismut-Antimon-Dotierungselement-Legierungsschicht (50; 200), BiSbE-Legierungsschicht, über dem Substrat, wobei die BiSbE-Legierungsschicht eine (012)-Orientierung aufweist, wobei die BiSbE-Legierungsschicht Folgendes beinhaltet:

      Bismut;
      Antimon; und
      ein Dotierungselement,
      wobei das Bismut und Antimon der BiSbE-Legierungsschicht eine Vielzahl von BiSb-Lamellenschichten (210) bilden,
      wobei das Dotierungselement der BiSbE-Legierungsschicht eine oder mehrere Dotierungselement-Lamellenschichten (220) bildet,
      wobei jede der Dotierungselement-Lamellenschichten ein Material beinhaltet, das aus einer Gruppe ausgewählt ist, die aus einem nicht metallischen Dotierungselement,
      einem metallischen Dotierungselement und Kombinationen davon besteht, und
      wobei die BiSbE-Legierungsschicht die eine oder die mehreren Dotierungselement-Lamellenschichten an einem unteren Rand der BiSbE-Legierungsschicht beinhaltet.

2. SOT-Vorrichtung gemäß Anspruch 1, wobei das metallische Dotierungselement aus einer Gruppe ausgewählt ist, die aus Ni, Co, Fe, CoFe, NiFe, NiCo, NiCu, CoCu, NiAg, CuAg, Cu, Al, Zn, Ag, Ga, In und Kombinationen davon besteht.

3. SOT-Vorrichtung gemäß Anspruch 1, wobei das nicht metallische Dotierungselement aus einer Gruppe ausgewählt ist, die aus Si, P, Ge und Kombinationen davon besteht.

4. SOT-Vorrichtung gemäß Anspruch 1, wobei die BiSbE-Legierungsschicht das Dotierungselement in einer Konzentration von 0,5 Atom-% bis 15 Atom-% beinhaltet.

5. SOT-Vorrichtung gemäß Anspruch 1, wobei die BiSbE-Legierungsschicht $Bi_{1-x}Sb_xE$ beinhaltet, wobei x $0,05 < x < 0,22$ ist.

6. SOT-Vorrichtung gemäß Anspruch 1, wobei die BiSbE-Legierungsschicht mit einer Dicke von 20 Å bis 200 Å gebildet ist.

7. SOT-Vorrichtung gemäß Anspruch 1, wobei die BiSbE-Legierungsschicht ferner die eine oder die mehreren Dotierungselement-Lamellenschichten an einem oberen Rand

8. SOT-Vorrichtung gemäß Anspruch 1, wobei das Dotierungselement der BiSbE-Legierungsschicht eine Vielzahl von Dotierungselement-Lamellenschichten bildet und wobei die BiSbE-Legierungsschicht ferner die Dotierungselement-Lamellenschichten auf eine modulierte Weise in der BiSbE-Legierungsschicht gestapelt beinhaltet.

9. SOT-Vorrichtung gemäß Anspruch 1, wobei die BiSbE-Legierungsschicht ferner die eine oder die mehreren Dotierungselement-Lamellenschichten in der gesamten BiSbE-Legierungsschicht beinhaltet.

10. Ein Schreibkopf für energieunterstützte magnetische Aufzeichnung, EAMR, auf SOT-Basis, der die SOT-Vorrichtung gemäß Anspruch 1 beinhaltet, wobei die BiSbE-Legierungsschicht (50) in der Nähe einer Spin-Drehmoment-Schicht (60) liegt.

11. Eine Vorrichtung mit magnetoresistivem Direktzugriffsspeicher, MRAM, die die SOT-Vorrichtung gemäß Anspruch 2 beinhaltet, wobei die SOT-Vorrichtung ferner mindestens eine ferromagnetische Schicht (80, 88) mit senkrechter magnetischer Anisotropie, PMA, beinhaltet.

12. MRAM-Vorrichtung gemäß Anspruch 11, wobei die BiSbE-Legierungsschicht (50) eine Spin-Orbit-Materialelektrode in der Nähe einer Schicht (80) mit freier PMA ist.

13. MRAM-Vorrichtung gemäß Anspruch 11, wobei die ferromagnetische PMA-Schicht eine ferromagnetische Schicht (88) mit Referenz-PMA ist, wobei die ferromagnetische Schicht mit Referenz-PMA eine magnetische Richtung aufweist, die durch Ausglühen bei 270 °C oder darüber für zwei Stunden oder länger festgelegt wird.

14. MRAM-Vorrichtung gemäß Anspruch 13, wobei die BiSbE-Legierungsschicht (50) eine Rauigkeit, R_a, von 14 Å oder weniger aufweist, nachdem die ferromagnetische Schicht (88) mit Referenz-PMA ausgeglüht wurde.

15. MRAM-Vorrichtung gemäß Anspruch 11, wobei die BiSbE-Legierungsschicht (50) eine starke (012)-Textur aufzeigt und eine Rocking-Kurve von 11 Grad oder weniger aufweist.

16. MRAM-Vorrichtung gemäß Anspruch 13, wobei die BiSbE-Legierungsschicht (50) ein topologischer Isolator ist, nachdem die ferromagnetische Schicht (88) mit Referenz-PMA ausgeglüht wurde.

Revendications

1. Un dispositif de couple spin-orbite, SOT, (10) comprenant :

un substrat (20) ; et
une couche d'alliage bismuth-antimoine-élément dopant, BiSbE, (50 ; 200) par-dessus le substrat, la couche d'alliage BiSbE ayant une orientation (012), la couche d'alliage BiSbE comprenant,
du bismuth ;
de l'antimoine ; et
un élément dopant,
dans lequel le bismuth et l'antimoine de la couche d'alliage BiSbE forment une pluralité de couches lamellaires de BiSbE (210),
dans lequel l'élément dopant de la couche d'alliage BiSbE forme une ou plusieurs couches lamellaires d'élément dopant (220),
chacune des couches lamellaires d'élément dopant comprenant un matériau sélectionné dans un groupe constitué d'un élément dopant non métallique, d'un élément dopant métallique, et de combinaisons de ceux-ci, et
dans lequel la couche d'alliage BiSbE comprend les une ou plusieurs couches lamellaires d'élément dopant à un bord de dessous de la couche d'alliage BiSbE.

2. Le dispositif SOT de la revendication 1, dans lequel l'élément dopant métallique est sélectionné dans un groupe constitué de Ni, Co, Fe, CoFe, NiFe, NiCo, NiCu, CoCu, NiAg, CuAg, Cu, Al, Zn, Ag, Ga, In, et de combinaisons de ceux-ci.

3. Le dispositif SOT de la revendication 1, dans lequel l'élément dopant non métallique est sélectionné dans un groupe constitué de Si, P, Ge, et de combinaisons de ceux-ci.

4. Le dispositif SOT de la revendication 1, dans lequel la couche d'alliage BiSbE comprend l'élément dopant à une concentration allant de 0,5 % atomique à 15 % atomique.

5. Le dispositif SOT de la revendication 1, dans lequel la couche d'alliage BiSbE comprend $Bi_{1-X}Sb_XE$, x valant $0,05 < x < 0,22$.

6. Le dispositif SOT de la revendication 1, dans lequel la couche d'alliage BiSbE est formée jusqu'à avoir une épaisseur de 20 Å à 200 Å.

7. Le dispositif SOT de la revendication 1, dans lequel la couche d'alliage BiSbE comprend en outre les une ou plusieurs couches lamellaires d'élément dopant à un bord de dessus de la couche d'alliage BiSbE.

8. Le dispositif SOT de la revendication 1, dans lequel l'élément dopant de la couche d'alliage BiSbE forme une pluralité de couches lamellaires d'élément dopant et dans lequel la couche d'alliage BiSbE comprend en outre les couches lamellaires d'élément dopant empilées d'une manière modulée dans la couche d'alliage BiSbE.

9. Le dispositif SOT de la revendication 1, dans lequel la couche d'alliage BiSbE comprend en outre les une ou plusieurs

couches lamellaires d'élément dopant à travers la couche d'alliage BiSbE tout entière.

10. Une tête d'écriture d'enregistrement magnétique assisté par énergie, EAMR, à base de SOT, comprenant le dispositif SOT de la revendication 1, dans laquelle la couche d'alliage BiSbE (50) est à proximité d'une couche à couple de spin (60).

11. Un dispositif à mémoire vive magnétorésistive, MRAM, comprenant le dispositif SOT de la revendication 2, le dispositif SOT comprenant en outre au moins une couche ferromagnétique à anisotropie magnétique perpendiculaire, PMA, (80, 88).

12. Le dispositif MRAM de la revendication 11, dans lequel la couche d'alliage BiSbE (50) est une électrode de matériau spin-orbite à proximité d'une couche de PMA libre (80).

13. Le dispositif MRAM de la revendication 11, dans lequel la couche ferromagnétique PMA est une couche ferromagnétique PMA de référence (88), la couche ferromagnétique PMA de référence ayant une direction magnétique établie par un recuit de 270 °C ou au-delà pendant deux heures ou plus.

14. Le dispositif MRAM de la revendication 13, dans lequel la couche d'alliage BiSbE (50) a une rugosité, R_a, de 14 Å ou moins après que la couche ferromagnétique PMA de référence (88) a été recuite.

15. Le dispositif MRAM de la revendication 11, dans lequel la couche d'alliage BiSbE (50) montre une texture forte (012) et a une courbe oscillante de 11 degrés ou moins.

16. Le dispositif MRAM de la revendication 13, dans lequel la couche d'alliage BiSbE (50) est un isolant topologique après que la couche ferromagnétique PMA de référence (88) a été recuite.

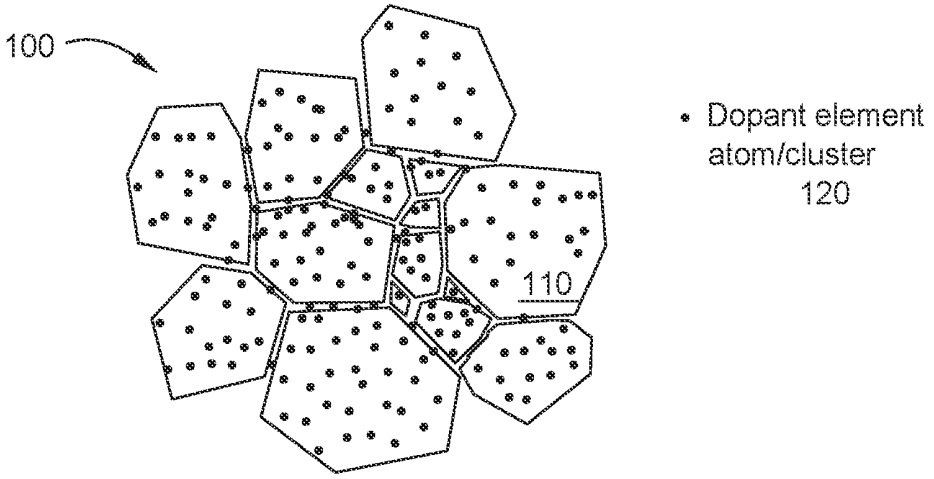

FIG. 1A

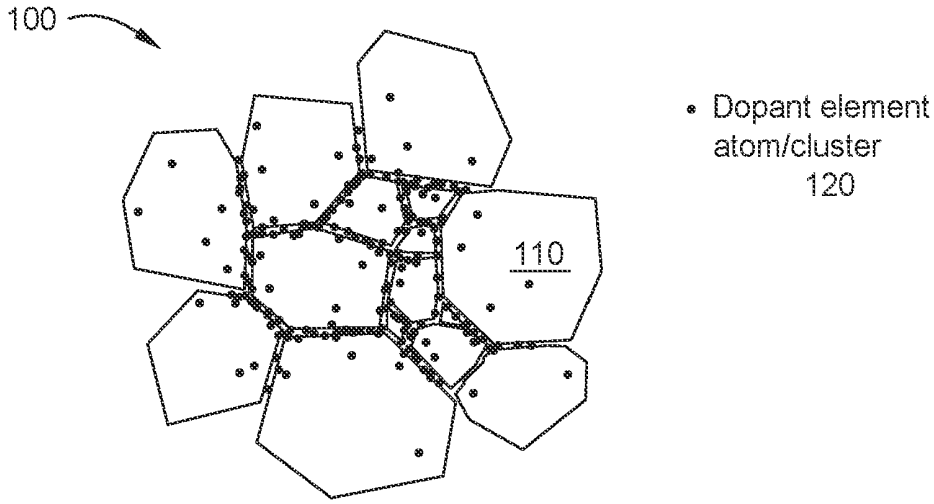

FIG. 1B

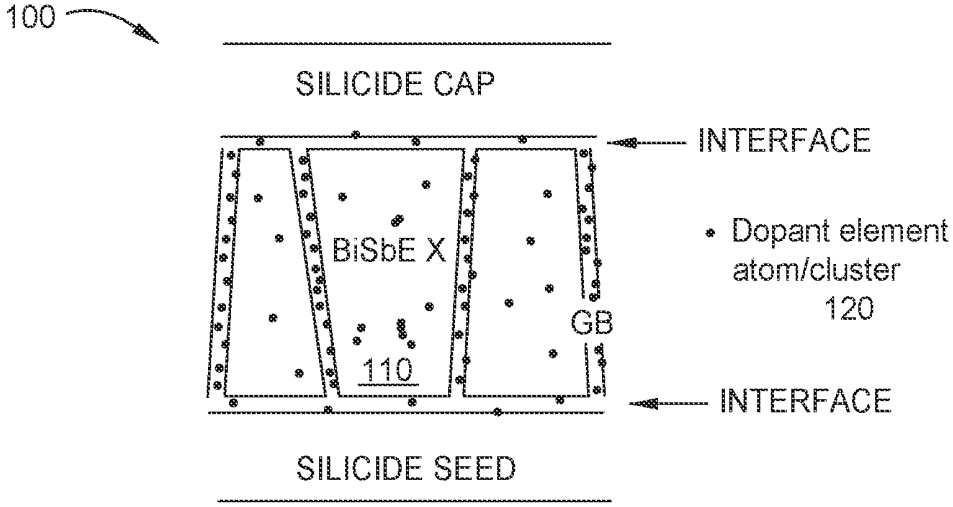

FIG. 1C

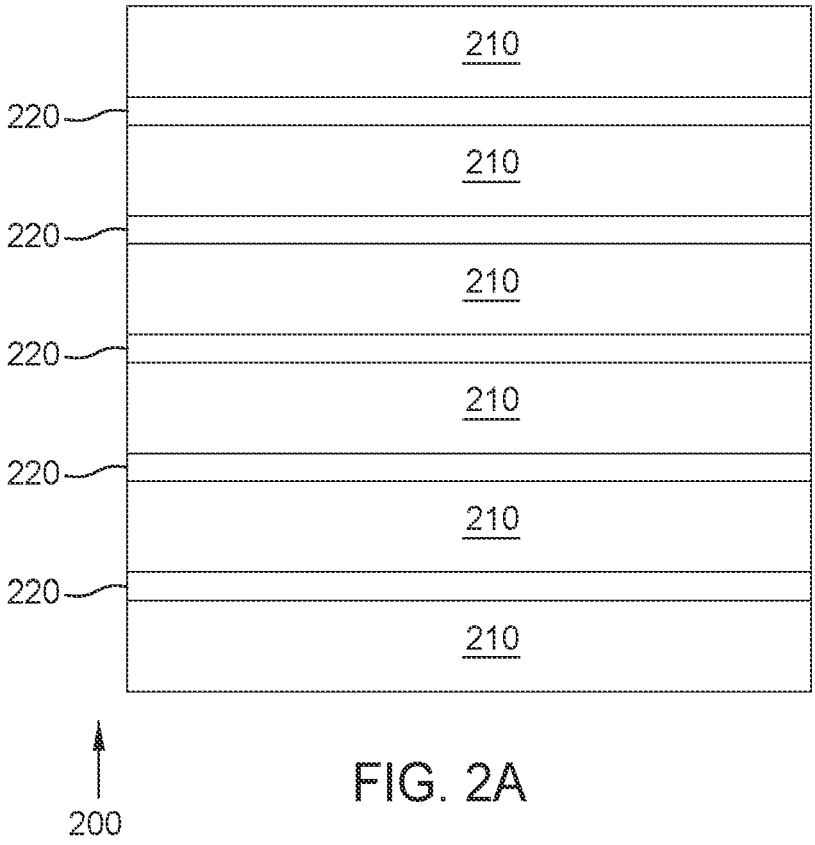
210
220
210
220
210
220
210
220
210
220
210
200

FIG. 2A

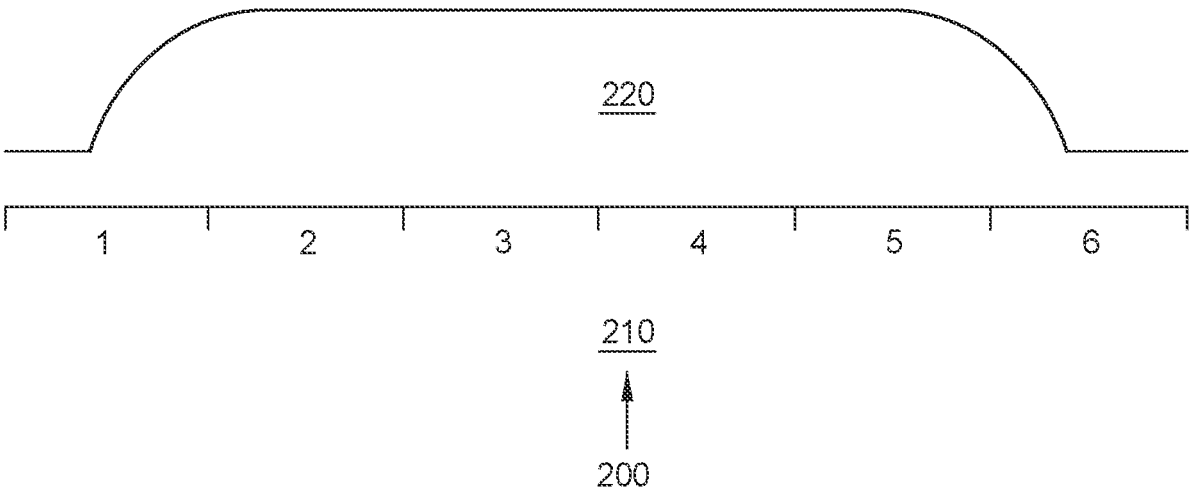
220
1
2
3
4
5
6
210
200

FIG. 2B

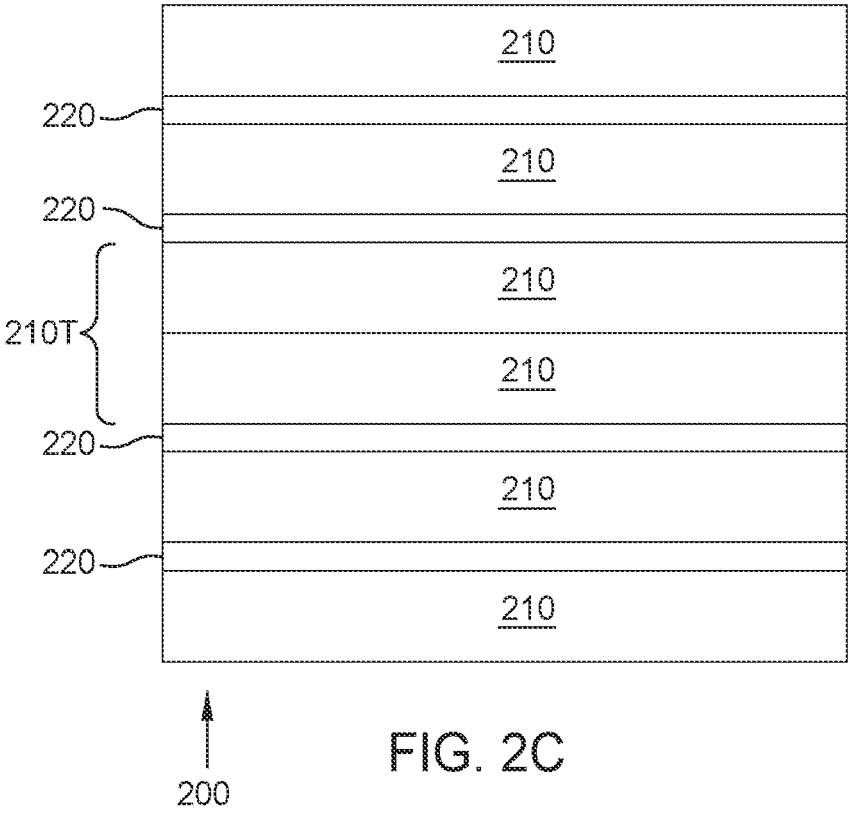
210
220
210
220
210T
210
210
220
210
220
210
200

FIG. 2C

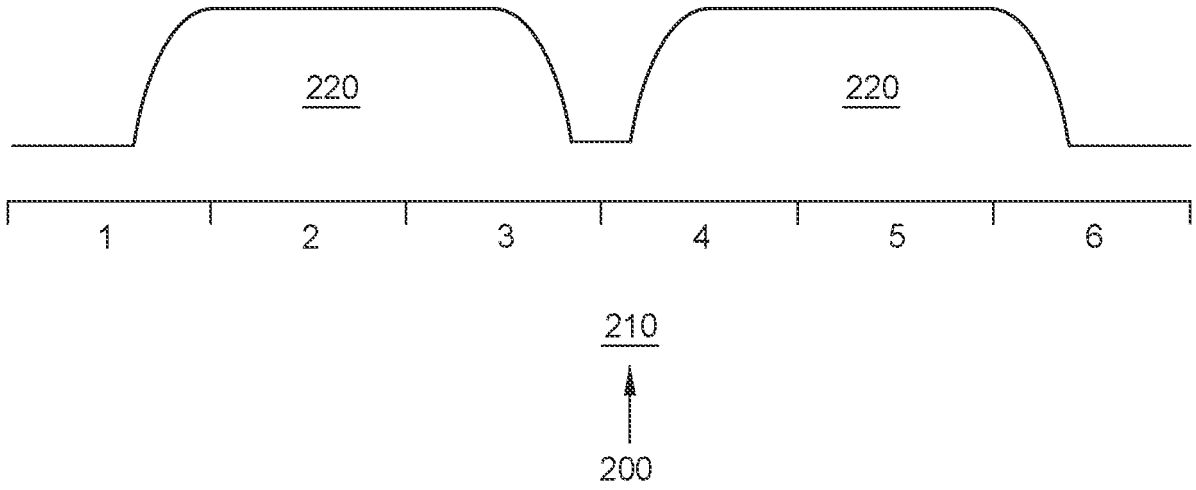
220
220
1
2
3
4
5
6
210
200

FIG. 2D

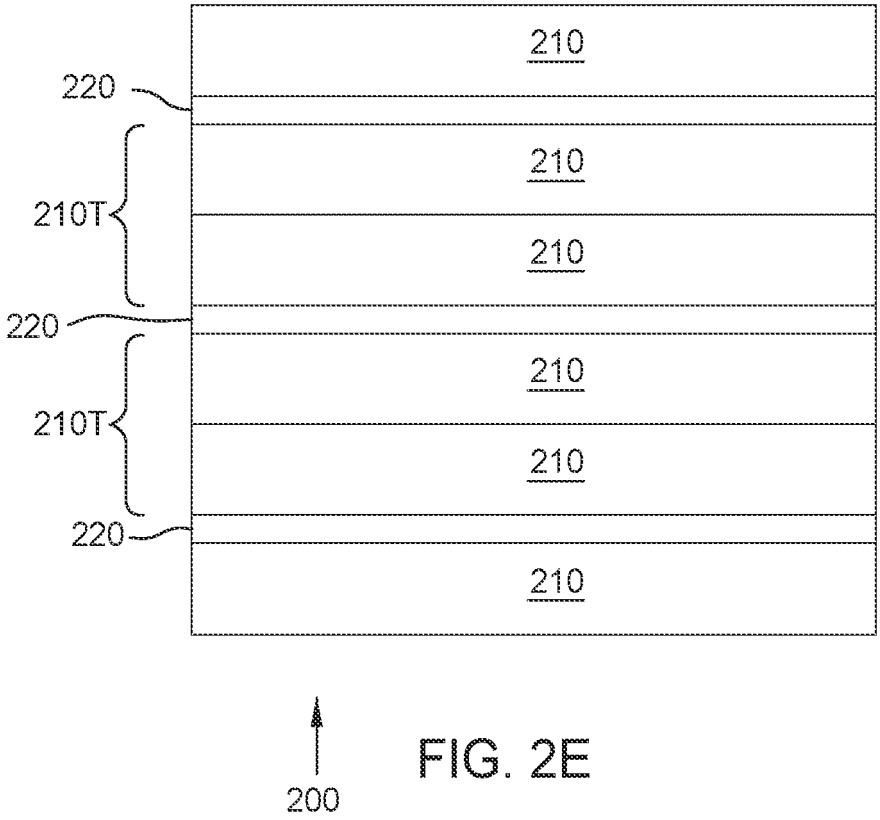
210
220
210
210T
210
220
210
210T
210
220
210
200

FIG. 2E

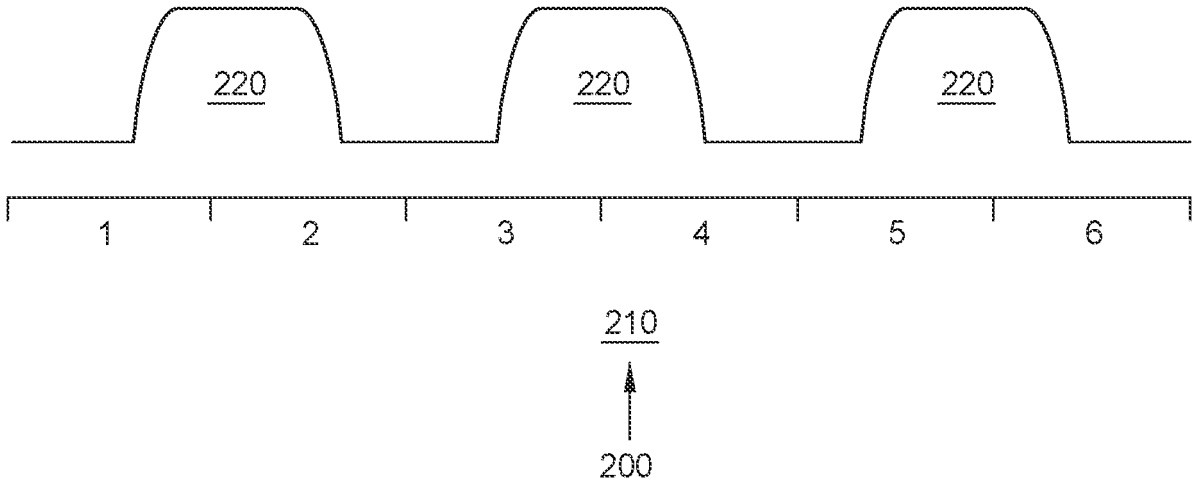
220
220
220
1
2
3
4
5
6
210
200

FIG. 2F

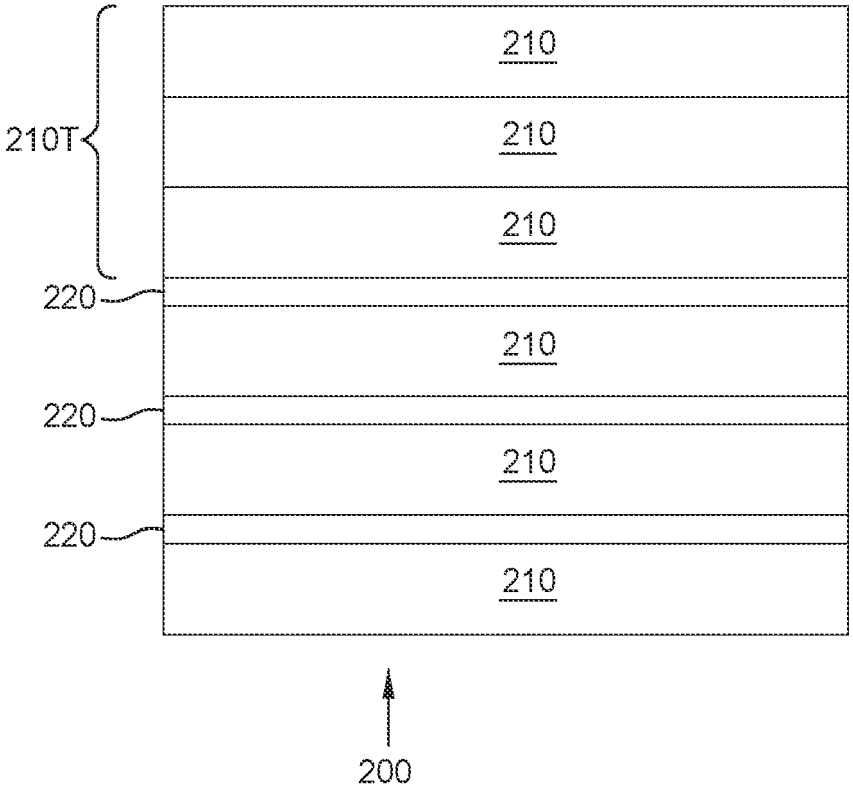

FIG. 2G

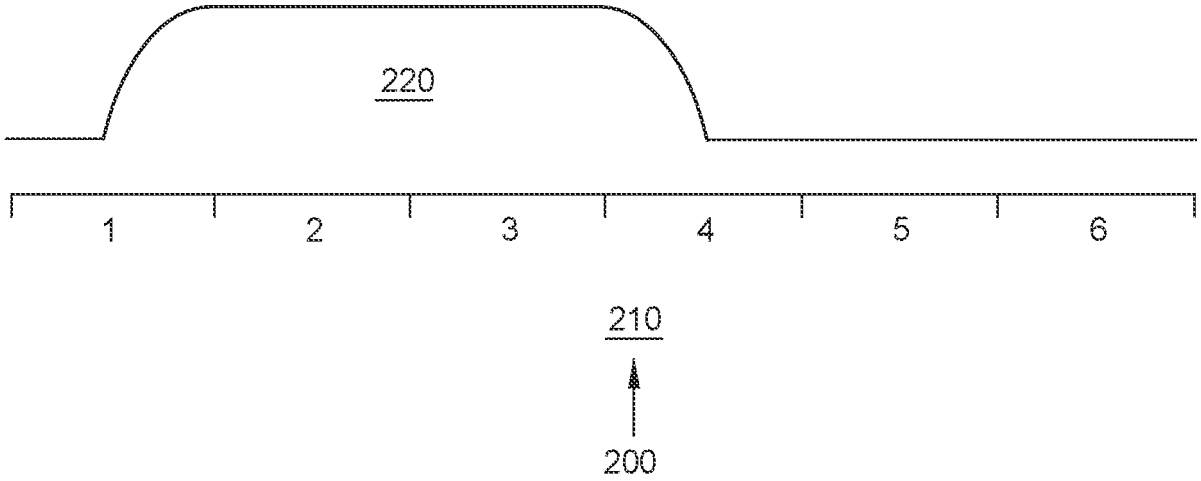

FIG. 2H

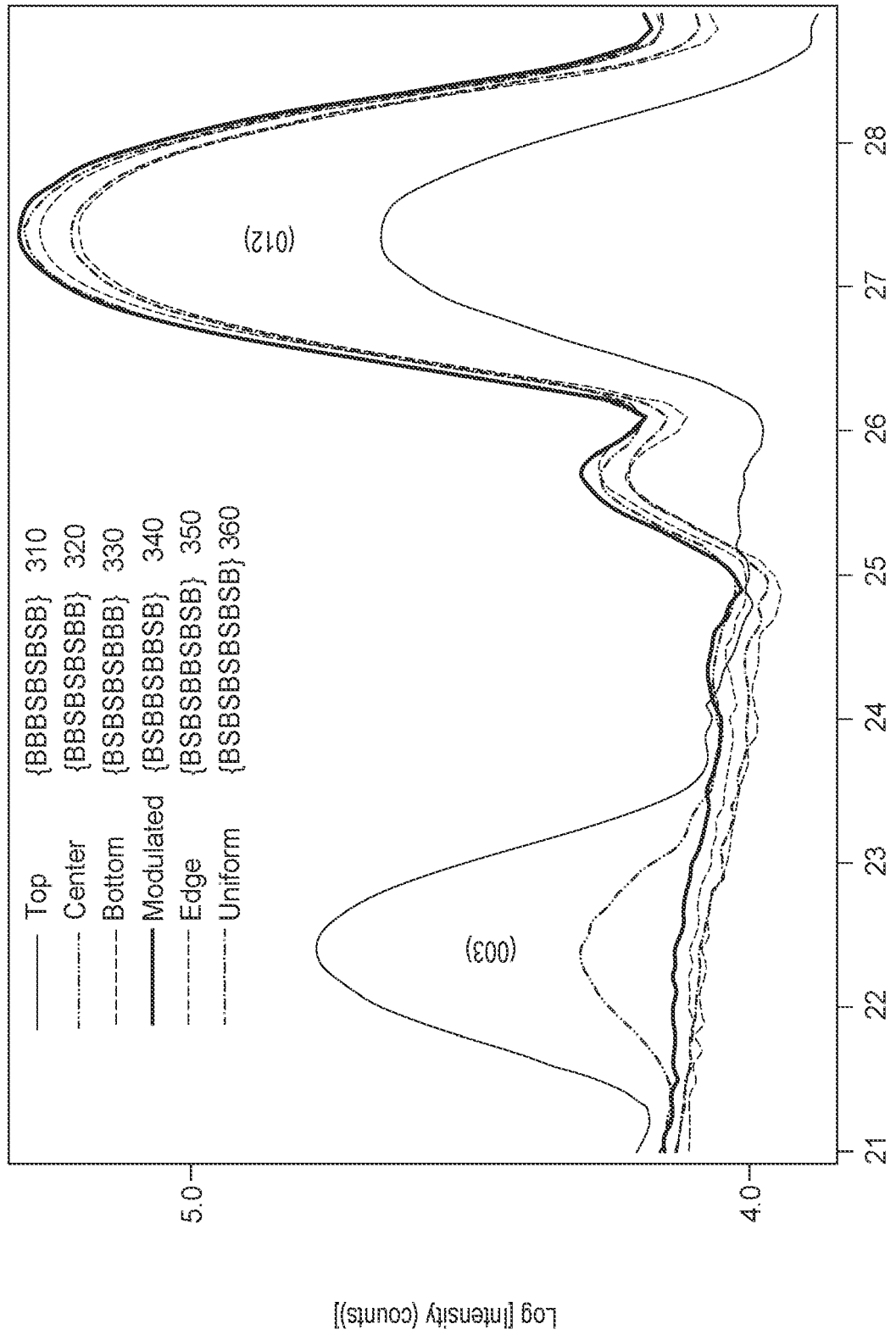
Top {BBBSBSBSB} 310
Center {BBSBSBSBB} 320
Bottom {BSBSBSBBB} 330
Modulated {BSBBSBBSB} 340
Edge {BSBSBBSBSB} 350
Uniform {BSBSBSBSBSB} 360
(003)
(012)
5.0
4.0
21
22
23
24
25
26
27
28
2θ (degs.)
Log [Intensity (counts)]

FIG. 3

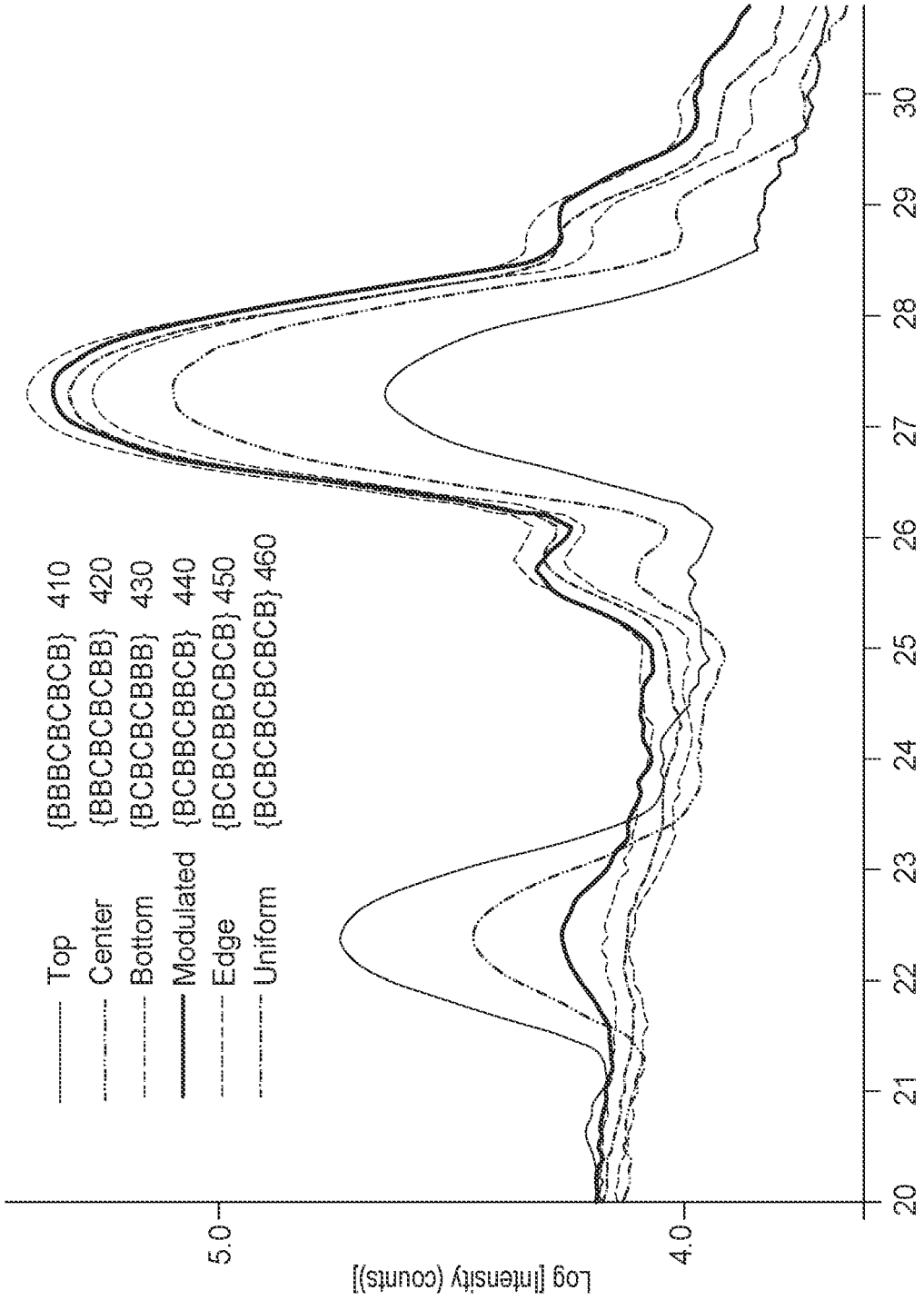
Top {BBBCBCBCB} 410
Center {BBCBCBCBB} 420
Bottom {BCBCBCBBB} 430
Modulated {BCBBCBBCB} 440
Edge {BCBCBBCBCB} 450
Uniform {BCBCBCBCBCB} 460
5.0
4.0
Log [Intensity (counts)]
20
21
22
23
24
25
26
27
28
29
30
2θ (degs.)

FIG. 4

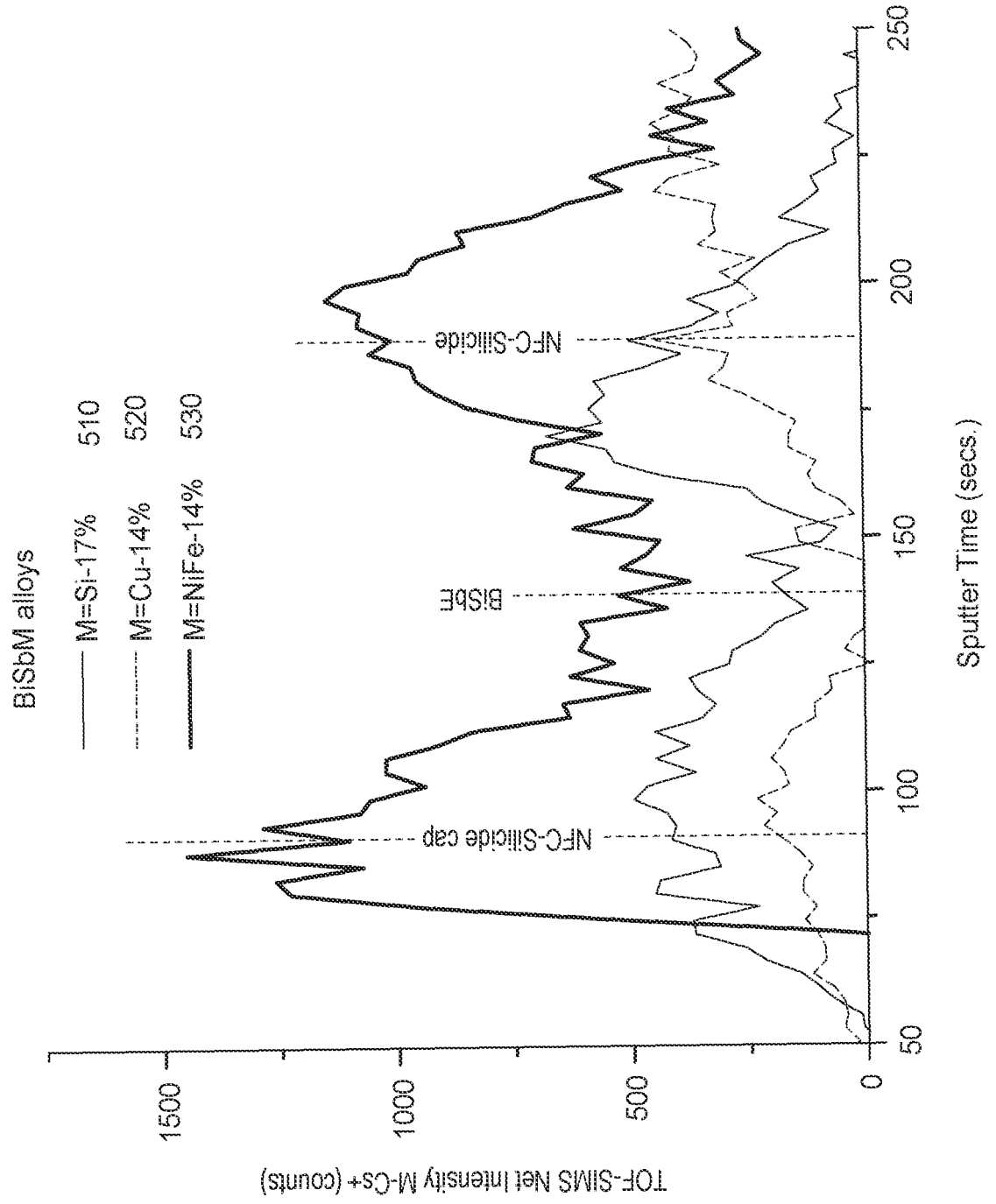
BiSbM alloys
M=Si-17%
510
M=Cu-14%
520
M=NiFe-14%
530
NFC-Silicide cap
BiSbE
NFC-Silicide
TOF-SIMS Net Intensity M-Cs+ (counts)
Sputter Time (secs.)
0
500
1000
1500
50
100
150
200
250

FIG. 5

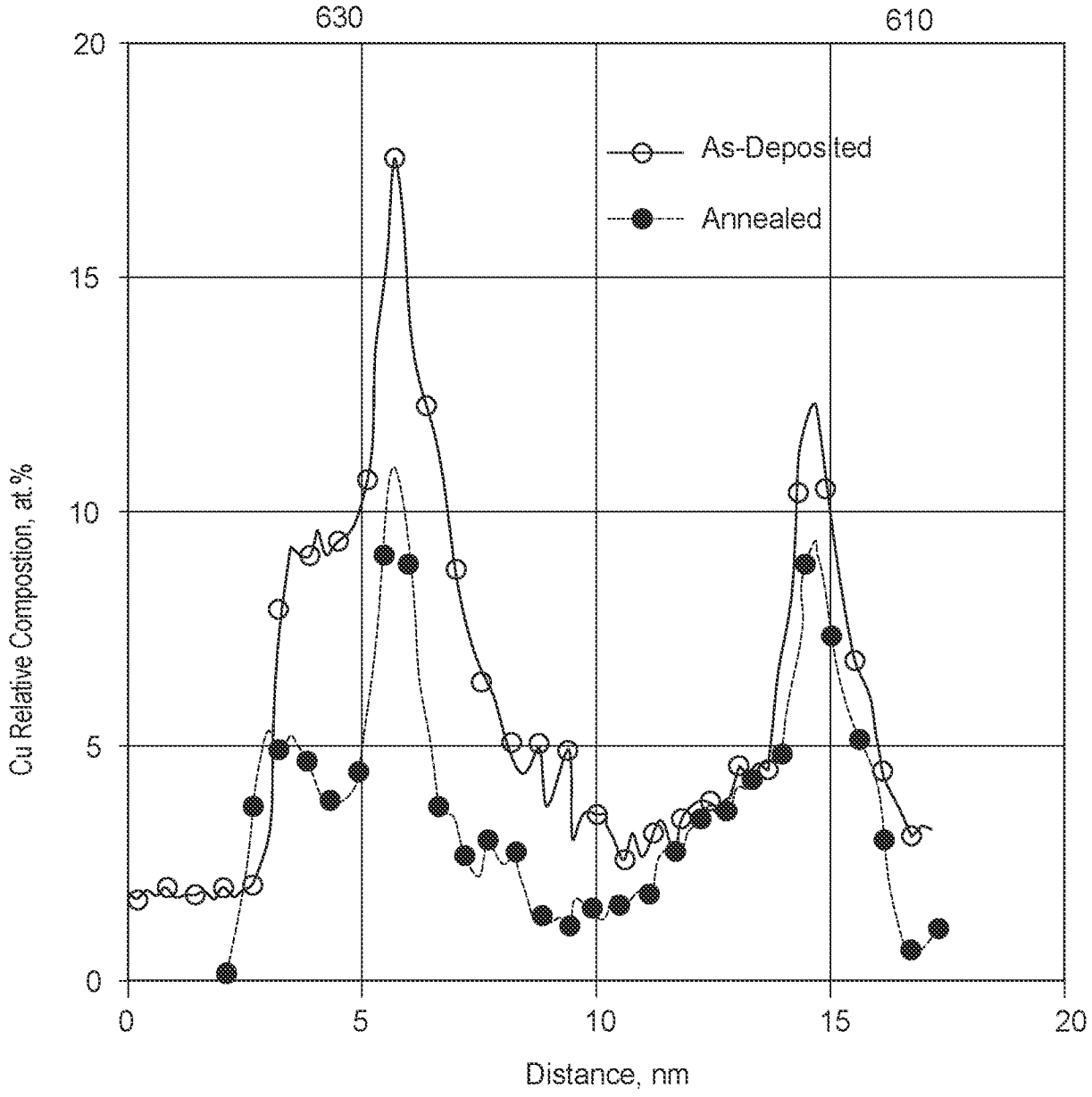
630
610
20
15
10
5
0
As-Deposited
Annealed
Cu Relative Compostion, at.%
0
5
10
15
20
Distance, nm

FIG. 6

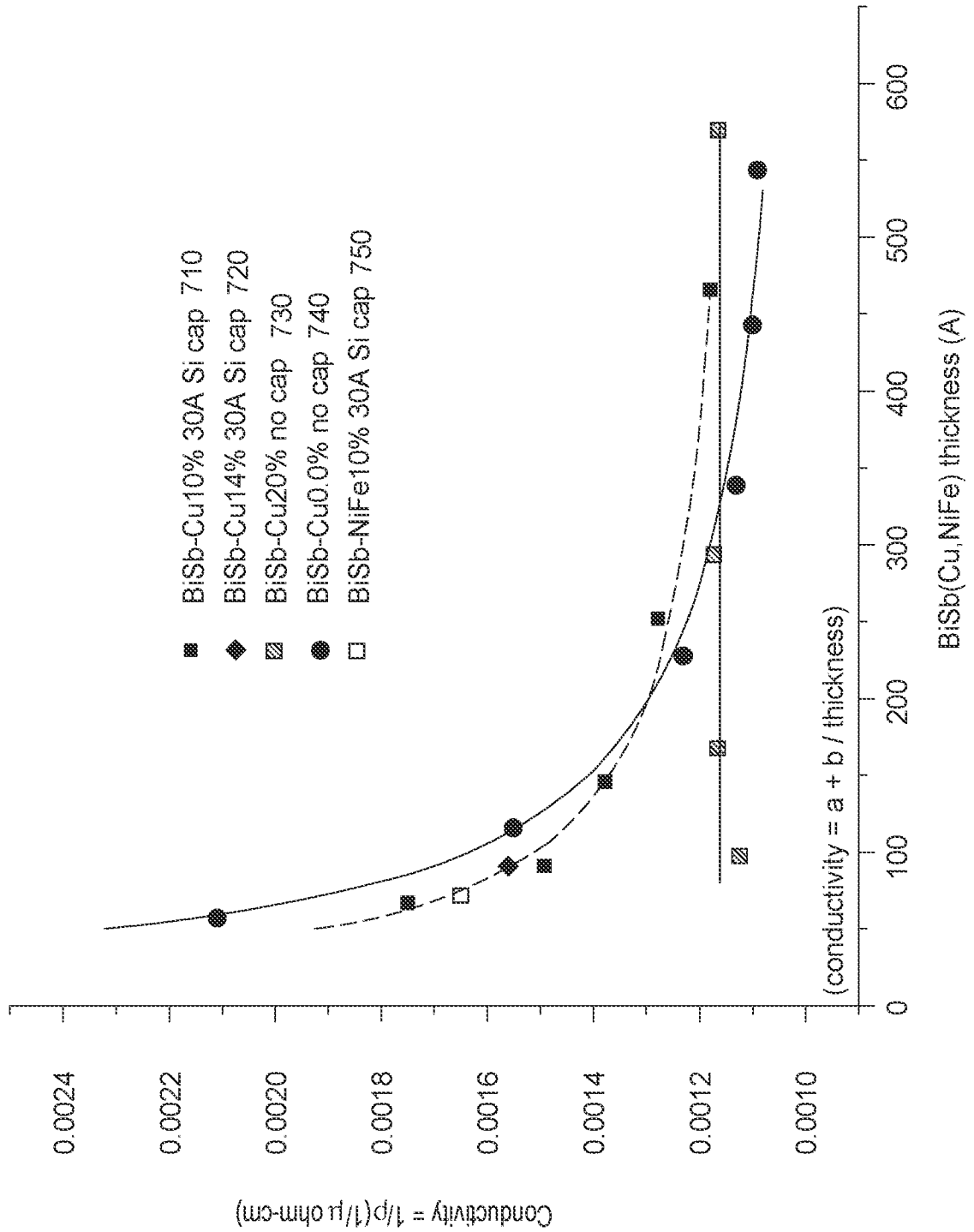
BiSb-Cu10% 30A Si cap 710
BiSb-Cu14% 30A Si cap 720
BiSb-Cu20% no cap 730
BiSb-Cu0.0% no cap 740
BiSb-NiFe10% 30A Si cap 750
(conductivity = a + b / thickness)
Conductivity = 1/ρ(1/μ ohm-cm)
0.0024
0.0022
0.0020
0.0018
0.0016
0.0014
0.0012
0.0010
0
100
200
300
400
500
600
BiSb(Cu,NiFe) thickness (A)

FIG. 7

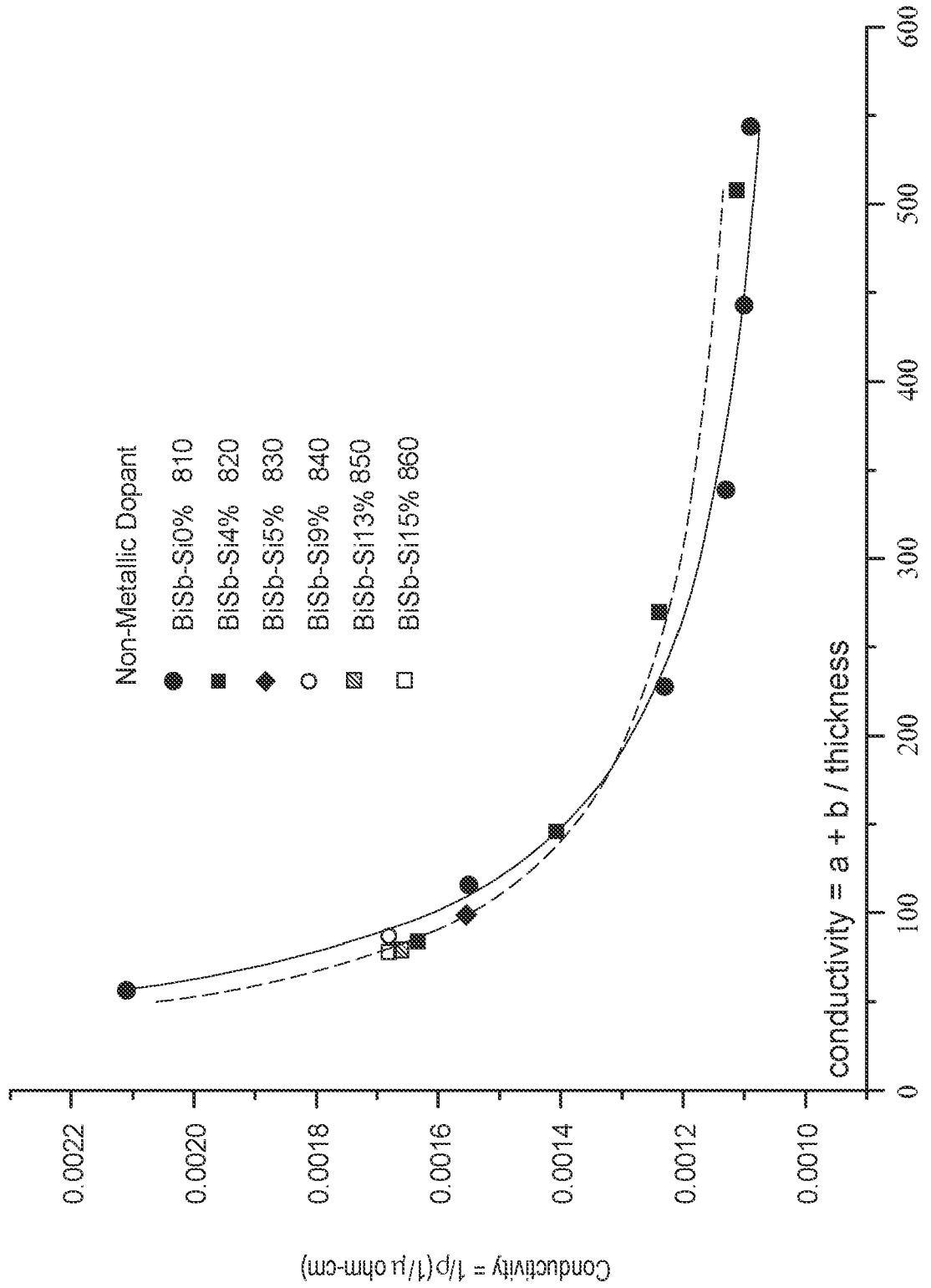
Non-Metallic Dopant
BiSb-Si0% 810
BiSb-Si4% 820
BiSb-Si5% 830
BiSb-Si9% 840
BiSb-Si13% 850
BiSb-Si15% 860
conductivity = a + b / thickness
Conductivity = 1/ρ(1/μ ohm-cm)
XRR Thickness(A)
0.0022
0.0020
0.0018
0.0016
0.0014
0.0012
0.0010
0
100
200
300
400
500
600

FIG. 8

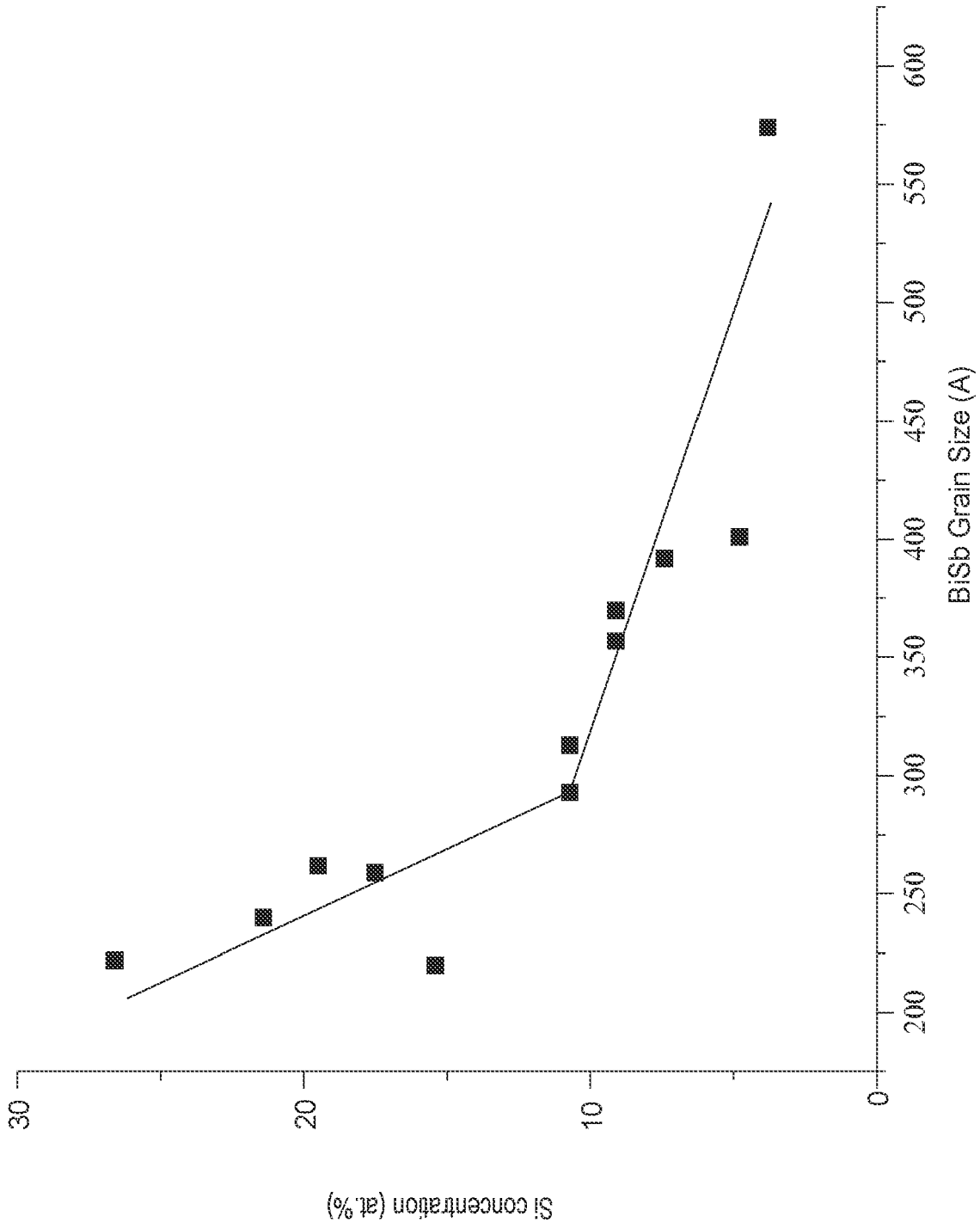
Si concentration (at.%)
0
10
20
30
200
250
300
350
400
450
500
550
600
BiSb Grain Size (A)

FIG. 9

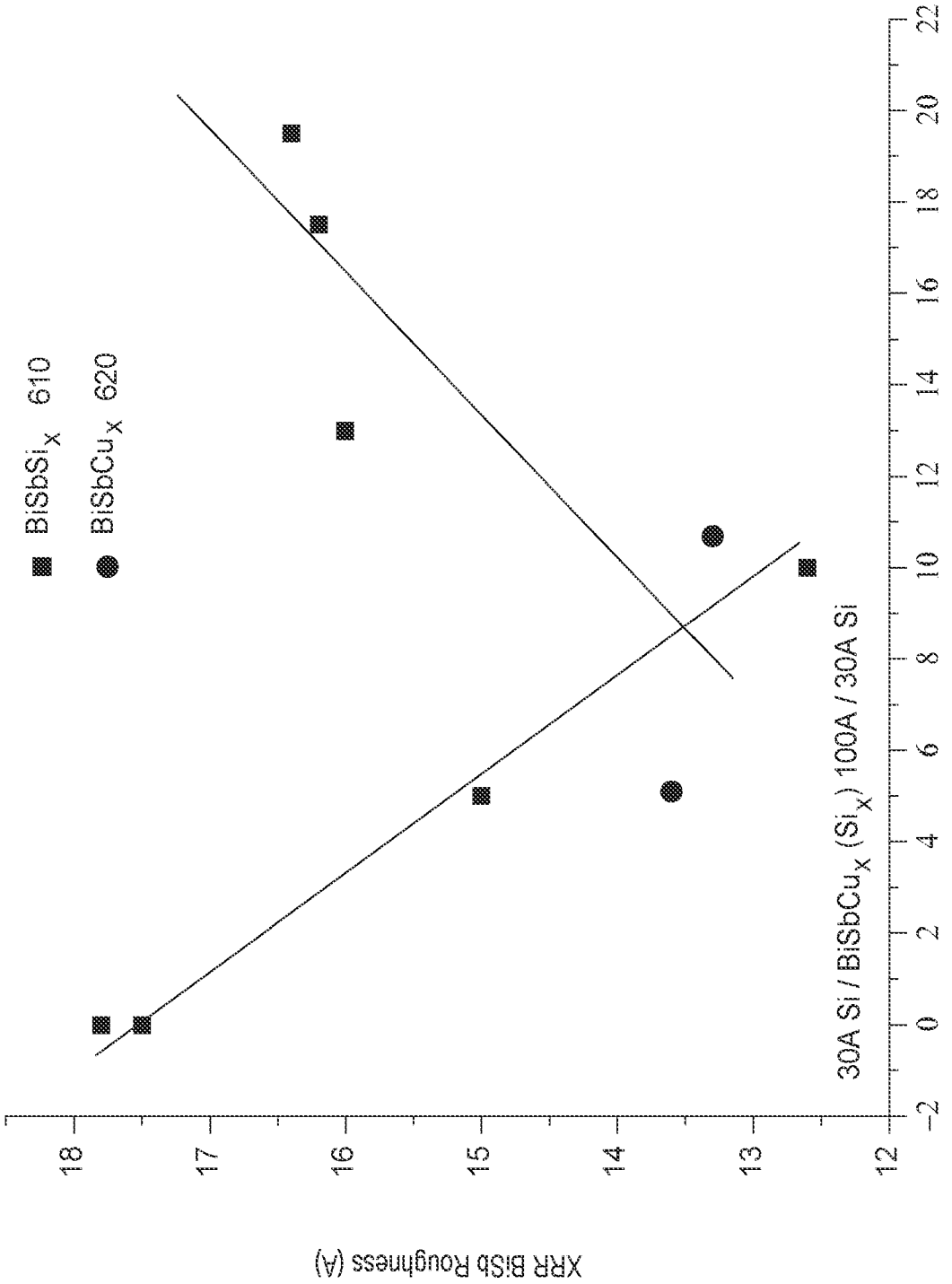
BiSbSi$_X$ 610
BiSbCu$_X$ 620
30A Si / BiSbCu$_X$ (Si$_X$) 100A / 30A Si
XRR BiSb Roughness (A)
X (at.%)
x
18
17
16
15
14
13
12
−2
0
2
4
6
8
10
12
14
16
18
20
22

FIG. 10

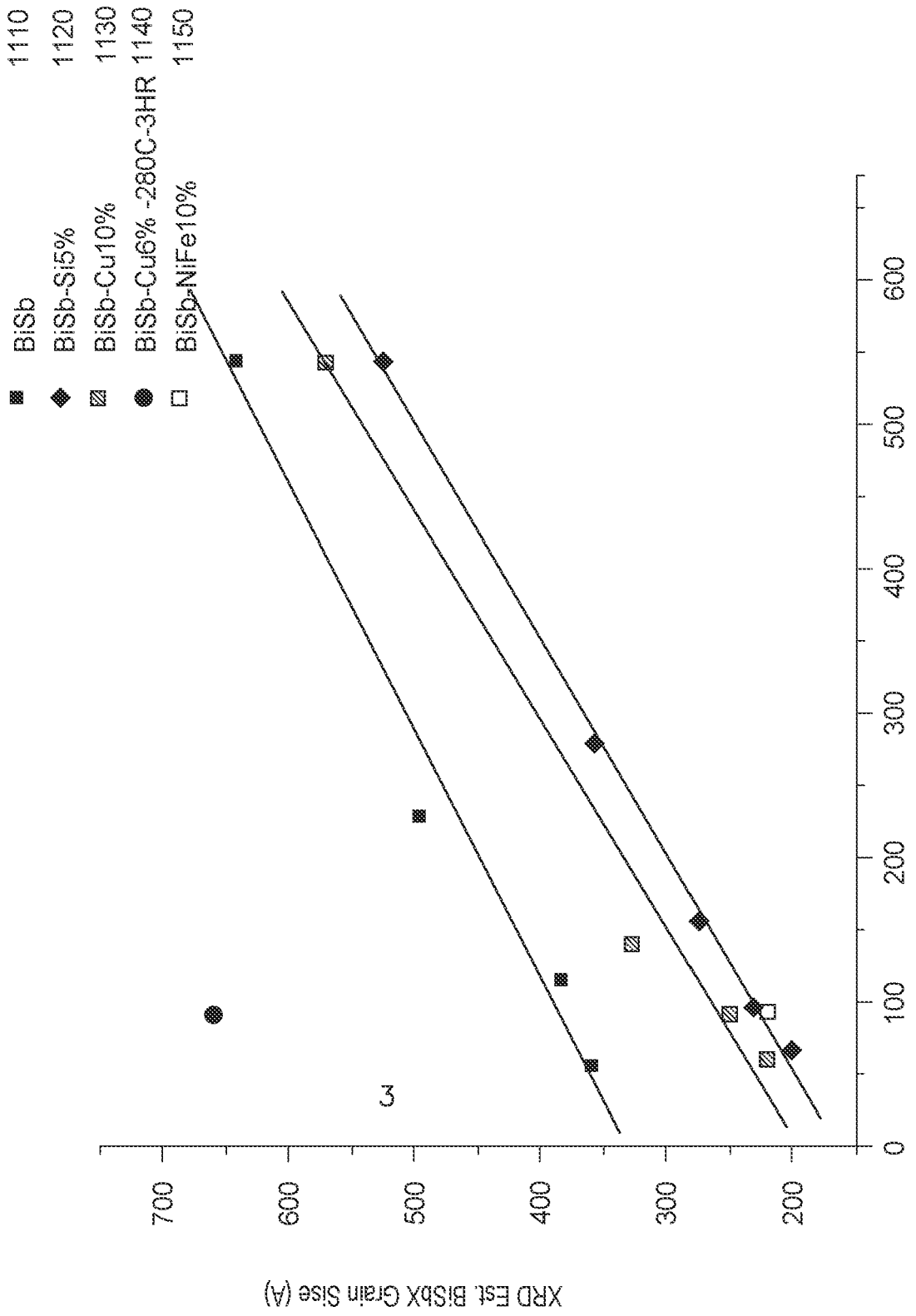
BiSb 1110
BiSb-Si5% 1120
BiSb-Cu10% 1130
BiSb-Cu6% -280C-3HR 1140
BiSb-NiFe10% 1150
XRD Est. BiSbX Grain Size (A)
BiSBbX Thickness (A)
0
100
200
300
400
500
600
200
300
400
500
600
700

FIG. 11

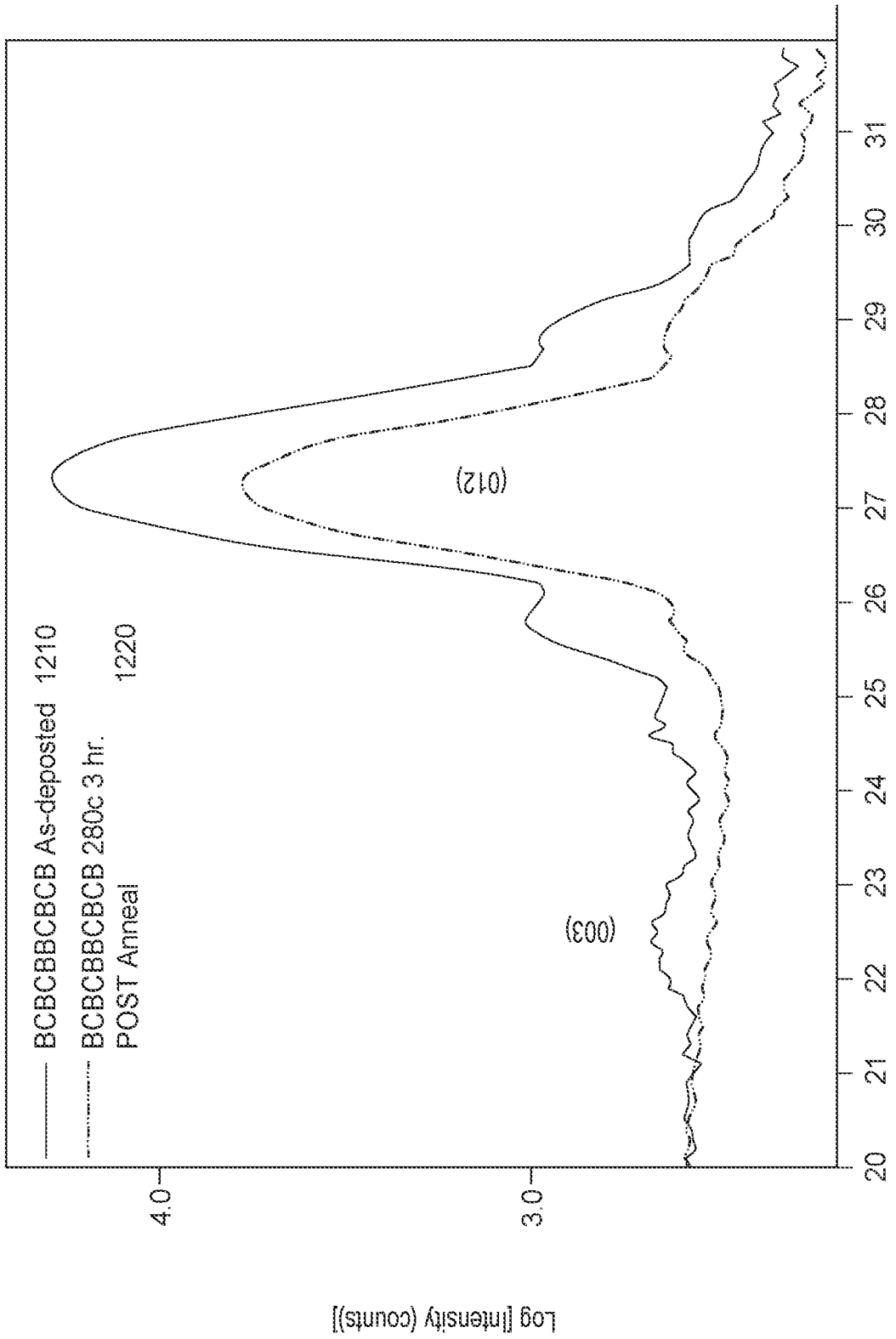
BCBCBBCBCB As-deposted 1210
BCBCBBCBCB 280c 3 hr. POST Anneal 1220
(003)
(012)
4.0
3.0
20
21
22
23
24
25
26
27
28
29
30
31
2θ (degs.)
Log [Intensity (counts)]

FIG. 12

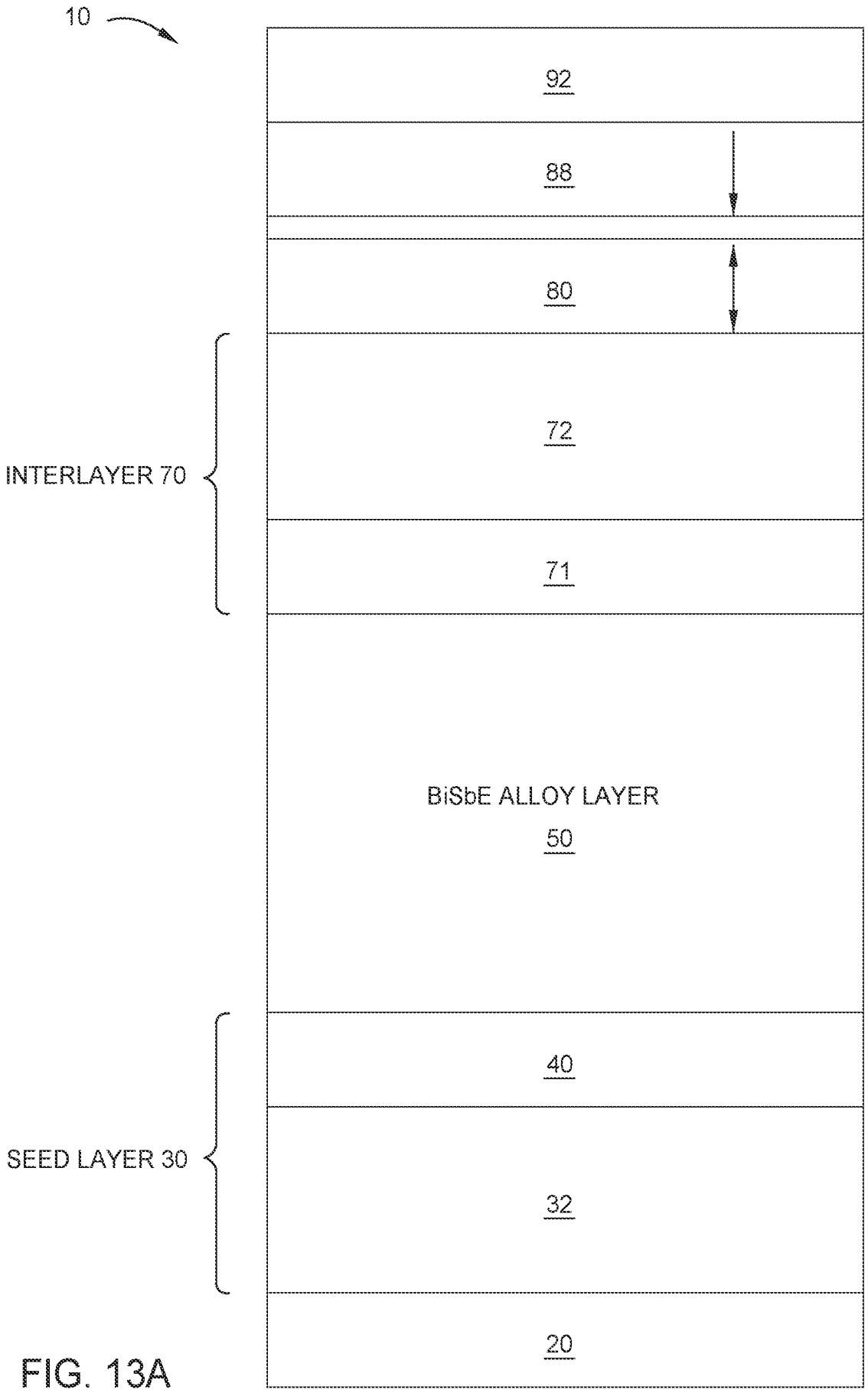
10
92
88
80
72
INTERLAYER 70
71
BiSbE ALLOY LAYER
50
40
SEED LAYER 30
32
20

FIG. 13A

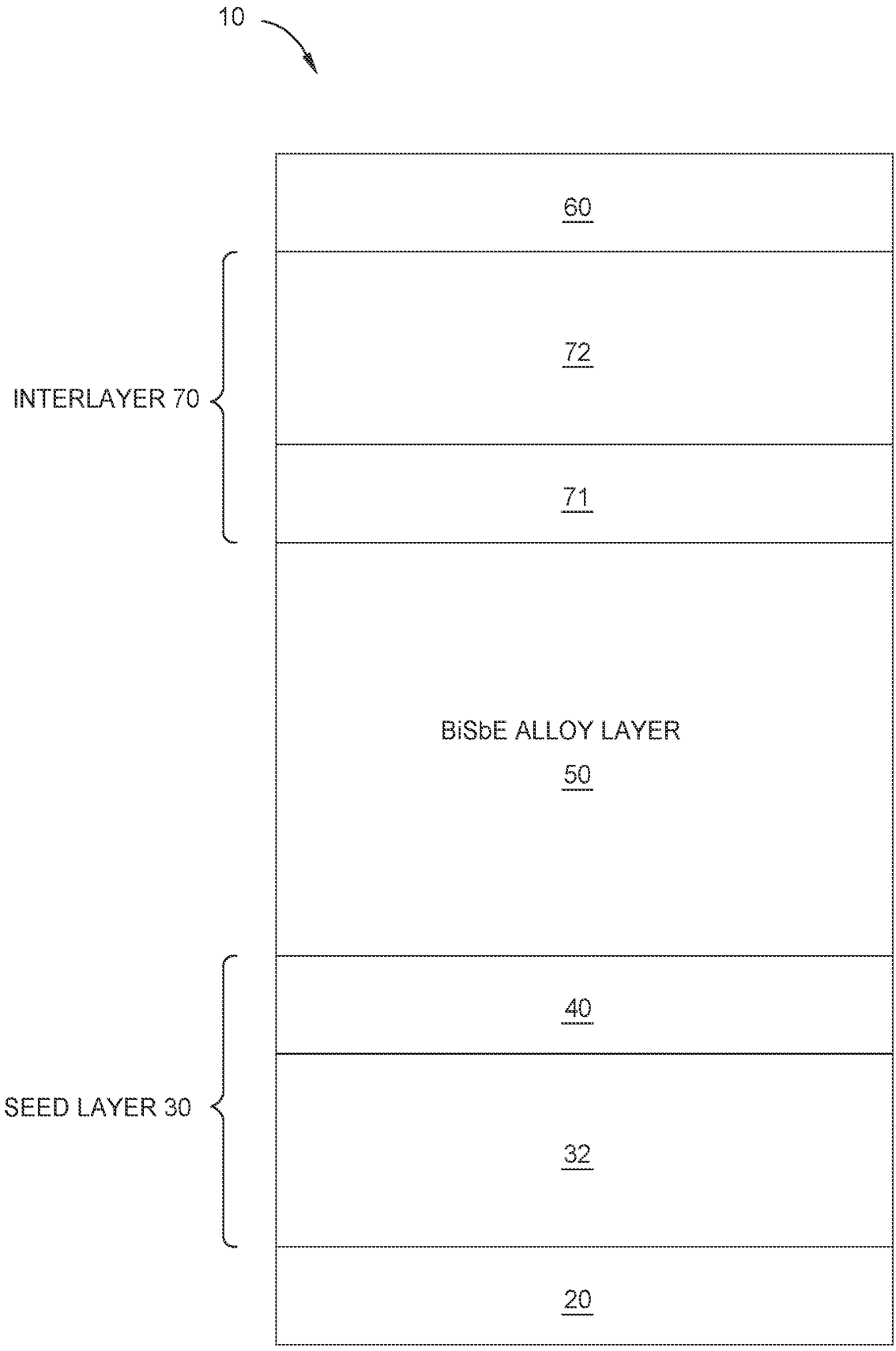
10
60
72
INTERLAYER 70
71
BiSbE ALLOY LAYER
50
40
SEED LAYER 30
32
20

FIG. 13B

REFERENCES CITED IN THE DESCRIPTION

This list of references cited by the applicant is for the reader's convenience only. It does not form part of the European patent document. Even though great care has been taken in compiling the references, errors or omissions cannot be excluded and the EPO disclaims all liability in this regard.

Patent documents cited in the description

- US 91733420 **[0001]**
- US 20170288666 A1 **[0007]**

Non-patent literature cited in the description

- **KHANG et al.** Conductive Topological Insulator With Large Spin Hall Effect For Ultralow Power Spin-Orbit Torque Switching. *Nature Materials*, 2018, vol. 17, 808-813 **[0008]**
- **TOKURA**. Magnetic Topological Insulators. *Nature Reviews Physics*, 2019, vol. 1, 126-143 **[0009]**